

Received April 27, 2021, accepted May 18, 2021, date of publication May 31, 2021, date of current version June 9, 2021.

Digital Object Identifier 10.1109/ACCESS.2021.3085002

# Prequalification Scheme of a Distribution System Operator for Supporting Wholesale Market Participation of a Distributed Energy Resource Aggregator

HEE SEUNG MOON<sup>1</sup>, (Student Member, IEEE), YOUNG GYU JIN<sup>2</sup>, (Member, IEEE),  
YONG TAE YOON<sup>1</sup>, (Member, IEEE), AND SEUNG WAN KIM<sup>3</sup>, (Member, IEEE)

<sup>1</sup>Electric Power Network Economics Laboratory, Department of Electrical and Computer Engineering, Seoul National University, Seoul 08826, Republic of Korea

<sup>2</sup>Power System Economics Laboratory, Department of Electrical Engineering, Jeju National University, Jeju-si 63243, Republic of Korea

<sup>3</sup>Smart Energy Network Design Laboratory, Department of Electrical Engineering, Chungnam National University, Daejeon 34134, Republic of Korea

Corresponding author: Seung Wan Kim (swakim@cnu.ac.kr)

This work was supported in part by the Korea Institute of Energy Technology Evaluation and Planning (KETEP) Grant funded by the Korean Government [Ministry of Trade, Industry, and Energy (MOTIE)] through the Development of Demonstration Zone for New Electricity Service Model under Grant 20194310100030, and in part by the Korea Electric Power Corporation (KEPCO) under Grant R17XA05-49.

**ABSTRACT** Increasing penetration of distributed renewable energy sources (DRESs) has resulted in the emergence of distributed energy resource aggregators (DERAs). A DERA participates in the transmission-level market operated by a transmission system operator (TSO), and the DERA's resources are connected to a jurisdiction of the distribution system operator (DSO). Inspired by the structure of the Korean power industry, this study assumes a minimal DSO that cannot directly dispatch the resources in its system. In this study, we develop a detailed procedure for prequalification wherein the DSO checks the DERA's bids that are submitted to the TSO markets. The proposed prequalification enables the DSO to secure the reliability of its system by providing limited network information to the DERA. The DERA modifies its bid until potential overvoltage and overflow problems are resolved, even in the worst case, including uncertainties. The proposed prequalification process is verified using the IEEE 33-bus distribution network. Compared to previous studies, the results demonstrate that the proposed prequalification can deal with distribution system constraints, even though uncertainties are included. The proposed prequalification process can be applied to power industries where the DSO does not have the full dispatch authority on DRESs.

**INDEX TERMS** Distribution system operator, prequalification process, distributed energy resource aggregator, optimal power flow, robust approach.

## I. INTRODUCTION

Distributed renewable energy sources (DRESs) are rapidly being dispersed into distribution systems [1]. Aggregated DRESs can create additional revenue streams by optimally scheduling and actively participating in transmission-level markets such as wholesale energy markets and balancing markets [2], [3]. The entity that aggregates multiple DRESs and submits an aggregate bid on the markets is generally called a distributed energy resource aggregator (DERA) [4]–[6]. On September 17, 2020, FERC issued Order 2222

The associate editor coordinating the review of this manuscript and approving it for publication was Ravindra Singh.

that enabled the participation of DRESs and DERAs in the wholesale energy market [7].

Because a DERA is not responsible for the reliability of distribution systems [8], an increase in the number of DRESs and DERAs can threaten the reliability of the passive distribution system [9], [10]. To manage the system, a distribution system operator (DSO) needs to utilize an advanced distribution management system (ADMS) that has functions such as data acquisition, control, state estimation, and power flow calculation. In addition to the ADMS, the DSO needs a distributed energy resource management system to manage multiple DRESs in its grid [11].

TABLE 1. TSO-DSO-DERA coordination models in several power markets.

Power market	Model of TSO-DSO coordination	Information exchanges between entities			Entity dispatching DERA
		TSO-DSO	DSO-DERA	TSO-DERA	
United Kingdom [12]	Current model (2017)	X	X	O	TSO
	Future model 1	O	O	$\Delta$ (via DSO)	DSO (with priority), TSO (second)
	Future model 2	O	O	O	TSO/DSO (jointly)
Japan [12]	Current model (2017)	O	X	$\Delta$ (via TO/DO)	TSO
	Future model	O	O	O	TSO
California ISO [12]	Current model (2016)	X	O	O	TSO, DO
	Future model	O	O	O	TSO, DSO
New York ISO [13]	Current model (2017)	O	X	O	TSO
	Future model 1	O	O	$\Delta$ (via DSO)	TSO (via DSO)
	Future model 2	O	O	O	TSO (directly)
SmartNet Project [14]	Centralized AS market model	O	O	O	TSO
	Local AS market model	O	O	$\Delta$ (via DSO)	DSO (with priority), TSO (second)
	Shared balancing responsibility model	O	O	O	DSO
	Common TSO-DSO AS market model	O	O	O	TSO/DSO (jointly)
	Integrated flexibility market model	$\Delta$ (via a third entity)	O	$\Delta$ (via a third entity)	A third entity

As the DERA participates in transmission-level markets, cooperative operation between the transmission system operator (TSO) and the DSO becomes essential. As the DERA submits a bid to the TSO, the TSO delivers dispatch signals to the DERA as a result of market and system operations.

In the conventional power system, because market participants of the TSO market are mainly located in the transmission level, the operating action of the TSO does not cause problems inside the distribution system. However, as the market participation of the DERA increases, the market clearing result may unintentionally threaten the reliability of the distribution system.

The cooperative operation procedure varies depending on the coordination process between the TSO and the DSO, which varies from country to country. Table 1 presents the current and future TSO-DSO coordination models in several power markets and the SmartNet project [12]–[14]. In the current environment, there are one or more missing points among the information links between the TSO-DSO, DSO-DERA, and TSO-DERA. However, future models have all the information links between TSO-DSO, DSO-DERA, and TSO-DERA [12]–[14]. Furthermore, in the current environment, only the TSO dispatches the DERA, but in the future models, a different entity controls the DERA depending on the TSO-DSO coordination. For example, in the current UK model, the TSO dispatches the DERA [12]. However, in UK future model 1, the DSO, which has priority over the TSO on the DERA’s bids, dispatches the DERA, and in UK future model 2, the TSO and DSO jointly control the DERA.

The different types of TSO–DSO coordination, including the authority of monitoring the distribution system and dispatching the DRESSs, can be categorized into centralized and decentralized approaches [15]. The centralized approach

represents the extension of the current TSO-centric power market into the distribution system and DRESSs. In the centralized approach, the TSO determines the activation of the DRESSs, while a minimal DSO cannot directly dispatch the DRESSs in its system. By contrast, in the decentralized approach, there is a total DSO that has more authority than the minimal DSO. The total DSO creates contracts with the TSO for the power flow at the point of common coupling and dispatches resources in its jurisdiction [16].

The two DSO models use different approaches to maintain reliability within each system. In the total DSO model, the DSO secures system security by directly controlling the resources of DERA. By contrast, in the minimal DSO model, the DSO is not authorized to control the resources of DERA directly; instead, the TSO controls the DERA’s resources. However, it is computationally demanding for the TSO to operate the entire system, including all the distribution systems [17], [18]. Thus, as an auxiliary means, a prequalification is necessary in the minimal DSO model. The prequalification is a process conducted by the DSO to examine whether a bid from its system threatens the system security or not [19]. As a result of the prequalification, the DSO can guide the DERA to resolve constraint violations, such as overflow and overvoltage [20].

Both DSO models are completely compatible in that each DSO can maintain a reliable distribution system and support the DERAs in participating in transmission-level markets or services. Compared to the total DSO model, the minimal DSO model and its prequalification process are more applicable option to current TSO markets as the TSO still determines the output of the DERAs. Also, it is easier to implement the minimal DSO model than the total DSO model in current TSO markets because of the power

industry structure. Therefore, in this paper, a minimal DSO that performs the prequalification process is proposed.

The remainder of this paper is organized as follows. Section II reviews the related academic literature. The role and responsibility of the TSO, DSO, and DERA are described in Section III. Details of the prequalification and formulations in each step are presented in Section IV. In Section V, the effectiveness of the proposed prequalification is verified using the IEEE 33-bus distribution network, with high penetration of DRESs. The conclusions obtained are presented in Section VI.

## II. LITERATURE REVIEW AND CONTRIBUTIONS

In the literature, there are three groups of papers that focus on the participation of DERAs in the wholesale market. The first group focused on the optimal bidding for a DERA. The second group concentrated on coordination between the TSO and DSO, and the third group concentrated on coordination between the DSO and DERA.

### A. LITERATURE FOCUSING ON THE DERA'S OPTIMAL BIDDING CONSIDERING UNCERTAINTIES

Many studies have proposed optimal bidding methodologies for a DERA considering the uncertainties of DRESs. In [21], Wang *et al.* proposed a price-responsive optimal bidding method in the real-time market, considering the uncertainty of wind turbines and photovoltaics. In [22], the gap decision theory was applied for the optimal bidding of a DERA to address uncertainties. In [23], Abapour *et al.* suggested a robust optimal bidding strategy using game theory, considering multiple DERAs. In [24], P. Sheikahmadi and S. Bahramara proposed a DERA as price maker in real-time market with a Bi-level approach. However, these studies did not consider the physical constraints of the distribution system.

### B. LITERATURE FOCUSING ON COORDINATION BETWEEN THE TSO AND DSO

Research on coordination between the TSO and DSO has mainly focused on the power flow on the TSO-DSO boundary [25]–[29]. In these studies, the main purpose of the DSO is to provide the TSO with economical and physically viable flexibility options. The DSO utilizes resources in its system to provide a flexibility service through the TSO-DSO boundary. The DSO calculates the feasible range of the only reactive power flexibility [25] or both the active and reactive power using optimal power flow (OPF) and Monte Carlo simulation [26]. In [27], Silva *et al.* presented an algorithm that uses OPF at multiple operating points; in [28], Riaz and Mancarella additionally considered ramping constraints. Furthermore, in [29], Gonzalez *et al.* included uncertainties from forecast errors. In [30], Sheikahmadi *et al.* considered both wholesale and local markets that are operated by TSO and DSO respectively. In these studies, coordination between the DSO and DERA is not the main issue. Thus, the total DSO model, which can control all resources in its system, is preferred.

### C. LITERATURE FOCUSING ON COORDINATION BETWEEN THE DSO AND DERA

The type of TSO-DSO coordination that determines whether it is a total DSO or minimal DSO also affects the manner in which the DSO and DERA interact. Under the total DSO model, the DSO directly dispatches DERA resources in its system [31]–[34]. In [31], Hu and Zhou included the congestion constraint in the dispatching scheme of a DSO. However, the voltage constraint was not considered because the DC optimal power flow method was used. In [32], Moutis *et al.* proposed the rule-based voltage regulation method, but congestion was not considered. In [33], Pudjianto *et al.* determined the optimal bidding problem of DERAs that included both voltage and congestion constraints. However, there was an impractical assumption that a commercial entity, i.e., the DERA, had all the distribution system information. Moreover, the effect of uncertainty on the distribution system was not considered. In [34], Fu *et al.* proposed a DSO that procured a reserve to deal with uncertainties from DRESs in its system.

In [35]–[37], intermediate DSOs that could dispatch only non-DERA resources were proposed. In [35], Park and Son proposed a DSO that could determine the aggregated power of the DERA to solve the voltage problem and a DERA that scheduled its resources to match the determined power. In [36], Lu *et al.* proposed an algorithm in which the DSO and DERA re-scheduled their resources while updating the Lagrange multiplier of the system constraints until the system constraints were resolved. By contrast, in [37], a DSO calculated the price at the node where the DERA was connected and delivered the price signal. However, there was a limitation that other resources should be dispatched first to determine the price. These studies [35]–[37] have the following common features: there is only a single point of connection between the DSO and each DERA, and problems caused by the uncertainty of DRESs are not considered from the perspective of the DSO.

In [38], [39], Koraki *et al.* proposed a minimal DSO that alleviated congestion in the distribution line by delivering constraints to the DERA, including sensitivity information. However, overvoltage problems were not considered in both studies. In [39], a DERA conducted stochastic-based optimal scheduling considering the uncertainty of DRESs. However, the method wherein the DSO could secure system safety against the uncertainty of DRESs was not considered. A summary of the papers is provided in Table 3.

### D. CONTRIBUTIONS OF THE STUDY

This study assumes a minimal DSO with limited functionality that is inspired by the current Korean power industry structure [34]. The minimal DSO cannot directly dispatch the active power output of the resources in its jurisdiction [40]. The merits of the proposed prequalification process are as follows:

- The process enables the minimal DSO to operate its system in a robust manner by considering the uncertainties

TABLE 2. Comparison of literature regarding coordination between DSO and DERA.

Ref.	DSO type	Information that DSO gives to DERA to relieve system constraints	Constraints management		Uncertainty management
			Voltage	Congestion	
[31]	Total DSO	Dispatch signal	-	O	-
[32]	Total DSO	Rule-based voltage regulation	O	-	-
[33]	Total DSO	Dispatch signal	O	O	-
[34]	Total DSO	Dispatch signal	O	-	O
[35]	Intermediate DSO	Aggregated Dispatch signal	O	-	-
[36]	Intermediate DSO	Consensus	O	O	-
[37]	Intermediate DSO	Price signal	O	O	-
[38, 39]	Minimal DSO	Sensitivity constraints	-	O	-
This paper	Minimal DSO	Sensitivity constraints	O	O	O

O: the item is considered. - : The item is not considered

of the DERA’s bid. To ensure that the uncertainties do not result in overvoltages and overflows in the distribution system, the DSO creates constraints and sends them to the DERA. Subsequently, the DERA indirectly solves the chance constrained optimization, including the constraints received from the DSO.

- Under the prequalification process, the DERA does not share its bidding strategy with the DSO. Using the process, the DSO only obtains the DERA’s bids rather than an objective function or any constraints of the DERA’s resources.
- The DERA cannot identify the full state of the distribution system. Delivering the full state of the distribution system to a commercial entity is impractical [41]. Thus, the guidelines for the DERA do not include the full state of the distribution system in this study.

III. ENVIRONMENT SURROUNDING THE MINIMAL DISTRIBUTION SYSTEM OPERATOR

A. KOREAN POWER INDUSTRY STRUCTURE

The specific conditions used in this study are derived based on the structure of the Korean power industry. In the Korean power industry, a minimal DSO can exist [42]. The current structure of the Korean power industry is presented in Figure 1 [43]. The KEPCO owns the transmission and distribution system and runs a monopolistic retail business. It might be difficult for the KEPCO to be the total DSO in a neutral position if it maintains its monopoly in the retail business [40]. Therefore, it can be assumed that the DSO is unable to dispatch DRESs directly; however, the DSO is still responsible for the reliability of its system. The discussion is stemmed from the Korean case, but the proposed methodology is applicable to the countries or the markets where minimal DSO is implemented.

B. INTERACTIONS AMONG THE ENTITIES

Figure 2 illustrates the interactions among the entities, including the prequalification process of the DSO. It is assumed that a TSO does not have responsibility and visibility with respect to the distribution system, and a minimal DSO is

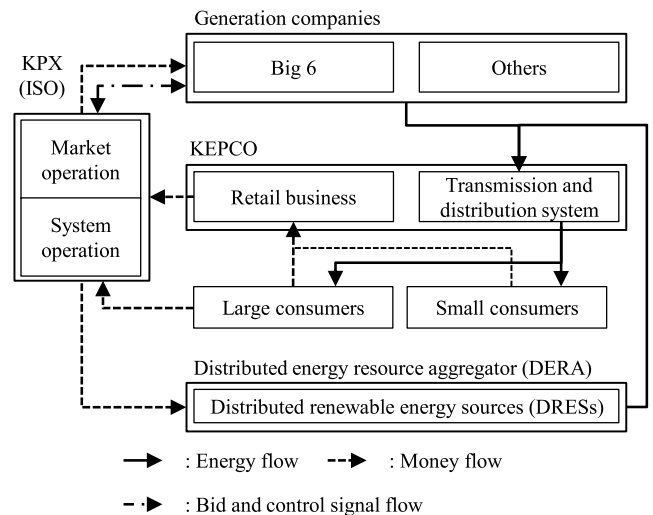


FIGURE 1. Schematic of the Korean power industry.

responsible for the reliability of its system. The distribution system with a large-scale penetration DRES is the subject of this study. However, the minimal DSO has limited authority in terms of dispatching the DRESs in its jurisdiction. A DERA participates in the wholesale energy market on behalf of the DRESs.

The DERA submits a bid to the DSO before participating in the market. If overvoltage or overflow problems are expected owing to the DERA’s bid on the distribution system, the DSO delivers bid-modification guidelines to the DERA for handling the potential problems. Subsequently, the DERA submits a modified bid following the guidelines. The process is repeated until no problem is expected, including uncertainties of demand and DERA’s bids. If the modified bid does not incur any violation, the bid is regarded as prequalified.

Moreover, the DERA can determine whether to submit the prequalified bid to the TSO or not. If the DERA is satisfied with the prequalified bid, it submits the bid to the TSO. Subsequently, the TSO includes the bid to the market offers and dispatches resources based on the bid. If the DERA is dissatisfied with the prequalified bid, it submits the bid to the DSO and undergoes the prequalification process again.

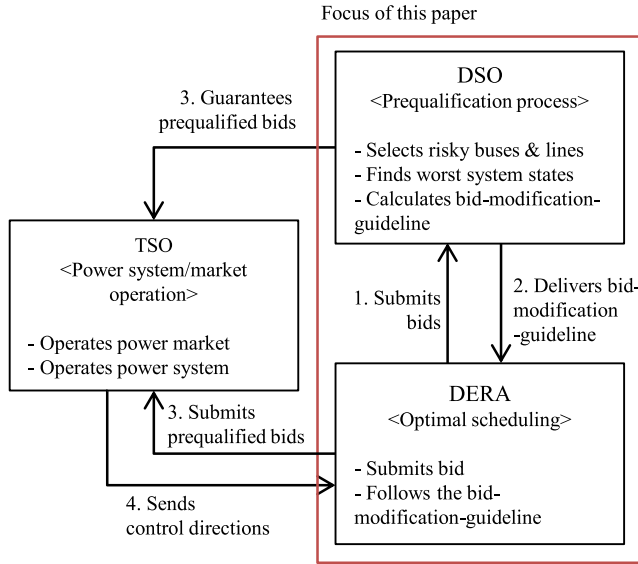


FIGURE 2. Interactions among the entities under the prequalification process by the DSO.

C. SOCIAL WELFARE MAXIMIZATION PROBLEM FOR DISTRIBUTION SYSTEMS

We assume a distribution system with the following conditions: 1) inflexible demands 2) zero-marginal-cost DRESs 3) a non-zero price generated from outside the distribution system 4) electricity customers and DRES producers as price takers.

In practice, most DSOs are regulated entities that they should be neutral and pursuing social welfare maximization. Thus, we assumed a DSO that maximizes social welfare in its distribution system. In the distribution system, social welfare can be defined as a sum of the customers' and producers' surplus. Because it is assumed that the customers are price takers with a inflexible demand, their surplus is constant. The producers are also assumed to be price takers, but their output depends on the physical constraints of the distribution system. Thus, the maximization of the DRES output in the distribution system can lead to a maximization of social welfare in the distribution system. Because DRES outputs have uncertainties, the social welfare maximization problem can be formulated in a chance-constrained problem as eq. (1):

$$\max_{\mathbf{x}} \mathbb{E} \left[ \sum_{i \in \mathcal{G}} \tilde{p}_{g,i} \right] \quad (1a)$$

$$\text{subject to } \tilde{p}_{g,i} = p_{g,i} \cdot \xi_{g,i}, \forall i \in \mathcal{G} \quad (1b)$$

$$\tilde{q}_{g,i} = q_{g,i} \cdot \xi_{g,i}, \forall i \in \mathcal{G} \quad (1c)$$

$$\tilde{P}_{d,i} = \tilde{P}_{d,i} \cdot \xi_{d,i}, \forall i \in \mathcal{N} \quad (1d)$$

$$\tilde{Q}_{d,i} = \tilde{Q}_{d,i} \cdot \xi_{d,i}, \forall i \in \mathcal{N} \quad (1e)$$

$$\Pr \left\{ |v_i(\xi)| \leq \bar{V}, \right\} \geq 1 - \epsilon, \quad \forall i \in \mathcal{N} \setminus \{1\} \quad (1f)$$

$$\Pr \left\{ |s_{f,l}(\xi)|^2 \leq \bar{S}_{f,l}^2 \right\} \geq 1 - \epsilon, \quad \forall l \in \mathcal{L} \quad (1g)$$

$$G(p_g, q_g, |v(\xi)|, |s_f(\xi)|, \mathbf{x}(\xi), \xi) \leq 0 \quad (1h)$$

$$H(p_g, q_g, |v(\xi)|, |s_f(\xi)|, \mathbf{x}(\xi), \xi) = 0 \quad (1i)$$

TABLE 3. Nomenclature.

Set and Indices	
$b, i, j, k$	Subscripts for buses
$l$	Subscripts for lines
$b_{rsk}, l_{rsk}$	Subscripts for risky bus and line
$s, \bar{s}$	Subscripts for iterations
$\mathcal{N}, \mathcal{L}, \mathcal{G}$	Set of bus, line, and DRES bus indexes
$\mathcal{N}_{rsk}, \mathcal{L}_{rsk}$	Set of risky bus and lines
$\mathcal{X}_{PF}^s, \mathcal{X}_V^s, \mathcal{X}_F^s, \mathcal{X}_S^s$	Set of the result of power flow, worst overvoltage state, worst overflow state, and optimal bidding by the DERA in iteration $s$
Parameters	
$nb, nl, ng$	The number of bus, line, and DRES buses
$G_{ij}, B_{ij}$	Conductance and susceptance of the line $l = (i, j)$ [p.u.]
$\bar{V}$	The upper limit of the voltage magnitude [p.u.]
$\bar{S}_{f,l}$	Rate capacity of line $l$ [MVA]
$\underline{pf}$	A lower limit of the power factor
$\bar{P}_{g,i}$	DRES output forecast [MW]
$\bar{P}_{d,i}, \bar{Q}_{d,i}$	Demand forecast [MW]
$\sigma_{d,i}^{high}, \sigma_{d,i}^{low}$	Upper and lower uncertainty range of demand forecast on bus $i$
$\sigma_{g,i}^{high}, \sigma_{g,i}^{low}$	Upper and lower uncertainty range of DRES output on bus $i$
$OV_i^s, OF_l^s$	Overvoltage and overflow violation on bus $i$ and line $l$ in iteration $s$ [p.u.]
$\epsilon_V, \epsilon_F, \epsilon_B$	Convergence criteria of overvoltage security, overflow security, and DERA bidding
$Sens_{vp,i,j}$	The sensitivity of voltage magnitude of bus $i$ to active power of bus $j$
$Sens_{vq,i,j}$	The sensitivity of voltage magnitude of bus $i$ to reactive power of bus $j$
$Sens_{sp,l,k}$	The sensitivity of squared complex flow of line $l$ to active power of bus $j$
$Sens_{sq,l,k}$	The sensitivity of squared complex flow of line $l$ to reactive power of bus $j$
Decision Variables	
$p_{g,i}, q_{g,i}$	Active and reactive power of a DERA bid on bus $i$ [MW, MVAR]
$\Delta p_{g,i}, \Delta q_{g,i}$	Adjustment of active and reactive power bid on bus $i$ [MW, MVAR]
$p_i, q_i$	Active and reactive injected power in bus $i$ [MW, MVAR]
$ v_i , \theta_i$	Magnitude and angle of voltage in bus $i$ [p.u., rad]
$s_{f,l}, p_{f,l}, q_{f,l}$	Complex, active, and reactive power flow in line $l$ [MVA, MW, MVAR]
Random Variables	
$\xi_{g,i}, \xi_{d,i}$	Forecast error for DRES output and demand

where  $\mathcal{G}, \mathcal{N}$ , and  $\mathcal{L}$  are the index sets of generator buses, load buses, and lines, respectively;  $\mathbf{p}_g$  and  $\mathbf{q}_g$  are the DRES outputs in bus  $i \in \mathcal{G}$ ;  $\mathbf{x} \in \mathbb{R}^{3nb+2nl}$  is a vector of decision variables that includes distribution system variables  $\mathbf{p}, \mathbf{q}, \boldsymbol{\theta}, \mathbf{p}_f$ , and  $\mathbf{q}_f$ ; and  $\boldsymbol{\xi} = [\boldsymbol{\xi}_g, \boldsymbol{\xi}_d] \in \mathbb{R}^{nb+ng}$  is a bounded random vector indicating forecast error of DRES outputs  $\boldsymbol{\xi}_g$  and that of demand  $\boldsymbol{\xi}_d$ . The letters in bold denotes a vector of variables that have the same letter, e.g.  $\mathbf{a}^s = [a_1^s, \dots, a_N^s]$ .  $G(\cdot)$  is the inequality constraint that includes the maximum DRES output constraint, and  $H(\cdot)$  is the equality constraint that includes the power balance equations. It is assumed that  $\boldsymbol{\xi}$  is bounded, i.e.,  $\boldsymbol{\xi} \in \{\boldsymbol{\xi} | \boldsymbol{\xi}^{min} \leq \boldsymbol{\xi} \leq \boldsymbol{\xi}^{max}\}$  and  $\mathbb{E}[\boldsymbol{\xi}] = \mathbf{1}$ .

Suppose that  $\mathbf{p}_g^*$  and  $\mathbf{q}_g^*$  are the solution of eq. (1); then, we obtain  $\boldsymbol{\xi}^{*,i}$  and  $\boldsymbol{\xi}^{*,l}$  that maximize  $|v(\boldsymbol{\xi})|$  and  $|s_f(\boldsymbol{\xi})|$  for each bus  $i$  and line  $l$ , respectively.  $\mathbf{p}_g^*$  and  $\mathbf{q}_g^*$  should satisfy eq. (1f, 1g) for most of the values of  $\boldsymbol{\xi}$  with a small  $\epsilon$ . The chance constraints in eq. (1f, 1g) can be reformulated into a

deterministic form, which is shown in eq. (2).

$$|v_i(\xi^{*,i})| \leq \bar{V}, \quad \forall i \in \mathcal{N} \setminus \{1\} \quad (2a)$$

$$|s_{f,l}(\xi^{*,l})| \leq \bar{s}_{f,l}^2, \quad \forall l \in \mathcal{L} \quad (2b)$$

However, the DERA is not qualified to access the network data because of security issues. Thus, the DSO runs the algorithm proposed in Section IV; this algorithm is called the prequalification process in this paper. If the DERA submits  $p_g^0$  and  $q_g^0$  with ignoring the system constraints represented in eq. (2), then the DSO calculates  $\xi^{*,i}$  and  $\xi^{*,l}$ , respectively.

Under the brute-force search method, the DSO must find  $nb$  scenarios that maximize the voltage on each bus and  $nl$  scenarios that maximize the line usage rate on each line. To find all values of  $\xi^{*,i}$  and  $\xi^{*,l}$  for each bus  $i$  and line  $l$ , respectively,  $nb+nl$  optimization problems need to be solved. Furthermore, the number of guidelines that the DSO delivers to the DERA is  $nb^2+nl^2$ . This approach is inefficient for both the DSO and the DERA because the DSO has to review a large number of scenarios, and the DERA has to include a large number of constraints. Moreover, a considerable amount of information must be transferred from the DSO to the DERA.

Instead, this study only finds a single worst case  $\xi^{v,rsk}$  and  $\xi^{f,rsk}$  for the overvoltage and overflow cases, respectively. The voltages in each bus are correlated to some extent, and the flows in each line are also correlated to some extent. These tendencies will be presented in the data in Section V-D. The worst overvoltage case,  $\xi^{v,rsk}$ , maximizes the sum of the voltage of the buses included in the risky bus set,  $\mathcal{N}_{rsk}$ . The worst overflow case,  $\xi^{f,rsk}$ , maximizes the sum of the line usage rate in the lines included in the risky line set,  $\mathcal{L}_{rsk}$ . The detailed method for determining  $\mathcal{N}_{rsk}$  and  $\mathcal{L}_{rsk}$  is presented in Section IV.

After  $\xi^{v,rsk}$  and  $\xi^{f,rsk}$  are determined,  $|v(\xi)|$  and  $|s_f(\xi)|^2$  can be linearly approximated at a point  $p_g^0, q_g^0, |v^0|, |s_f^0|, \xi^{v,rsk}$ , and  $\xi^{f,rsk}$  as a function of  $p_g$  and  $q_g$ , as shown in eq. (3).

$$\begin{aligned} &|V_i(p_g, q_g | \xi^{v,rsk})| \\ &= |v_i^0(\xi^{v,rsk})| + \nabla |v_i(\mathbf{p}^0, \mathbf{q}^0 | \xi^{v,rsk})|^T \\ &\quad \times (\mathbf{p} - \mathbf{p}^0, \mathbf{q} - \mathbf{q}^0), \quad \forall i \in \mathcal{N} \setminus \{1\} \end{aligned} \quad (3a)$$

$$\begin{aligned} &|S_{f,l}(p_g, q_g | \xi^{f,rsk})| \\ &= |s_{f,l}^0(\xi^{f,rsk})|^2 + \nabla [|s_{f,l}(\mathbf{p}^0, \mathbf{q}^0 | \xi^{f,rsk})|^2]^T \\ &\quad \times (\mathbf{p} - \mathbf{p}^0, \mathbf{q} - \mathbf{q}^0), \quad \forall l \in \mathcal{L} \end{aligned} \quad (3b)$$

where

$$\begin{aligned} \mathbf{p} &= p_g^T \xi_g^{rsk} - \bar{\mathbf{P}}_d^T \xi_d^{rsk}, & \mathbf{p}^0 &= p_g^{0,T} \xi_g^{rsk} - \bar{\mathbf{P}}_d^T \xi_d^{rsk}, \\ \mathbf{q} &= q_g^T \xi_g^{rsk} - \bar{\mathbf{Q}}_d^T \xi_d^{rsk}, & \mathbf{q}^0 &= q_g^{0,T} \xi_g^{rsk} - \bar{\mathbf{Q}}_d^T \xi_d^{rsk}, \end{aligned}$$

Subsequently, eq. (2) is replaced with a linearized function to derive eq. (4).

$$\begin{aligned} &|V_i(p_g, q_g | \xi^{v,rsk})| - \bar{V} \\ &= |v_i^0(\xi^{v,rsk})| - \bar{V} \end{aligned}$$

$$\begin{aligned} &+ \nabla [v_i(\mathbf{p}^0, \mathbf{q}^0 | \xi^{v,rsk})]^T (\mathbf{p} - \mathbf{p}^0, \mathbf{q} - \mathbf{q}^0) \\ &= OV_i + \nabla [v_i(\mathbf{p}^0, \mathbf{q}^0 | \xi^{v,rsk})]^T (\Delta \mathbf{p}, \Delta \mathbf{q}) \\ &\leq 0 \quad \forall i \in \mathcal{N} \setminus \{1\} \end{aligned} \quad (4a)$$

$$\begin{aligned} &|S_{f,l}(p_g, q_g | \xi^{f,rsk})| - \bar{s}_{f,l}^2 \\ &= |s_{f,l}^0(\xi^{f,rsk})|^2 - \bar{s}_{f,l}^2 \\ &+ \nabla [|s_{f,l}(\mathbf{p}^0, \mathbf{q}^0 | \xi^{f,rsk})|^2]^T (\mathbf{p} - \mathbf{p}^0, \mathbf{q} - \mathbf{q}^0) \\ &= OF_l + \nabla [|s_{f,l}(\mathbf{p}^0, \mathbf{q}^0 | \xi^{f,rsk})|^2]^T (\Delta \mathbf{p}, \Delta \mathbf{q}) \\ &\leq 0 \quad \forall l \in \mathcal{L} \end{aligned} \quad (4b)$$

where  $OV_i$  and  $OF_l$  are the constraint violations for each worst case  $\xi^{v,rsk}$  and  $\xi^{f,rsk}$ , respectively. By transferring eq. (4) as a guideline, the DSO can maximize the social welfare and increase security of the system. The detailed algorithm for the proposed method is presented in the following section.

#### IV. FORMULATIONS OF THE PREQUALIFICATION PROCESS

Figure 3 presents the flow chart of the proposed prequalification algorithm. Detailed formulations are described in the following subsections. It is assumed that the DERA submits active and reactive power bids,  $p_g^s$  and  $q_g^s$ , respectively, to the DSO before the prequalification process starts.

##### A. STEP 1: SELECTING A SET OF OVERVOLTAGE CANDIDATE BUSES AND A SET OF OVERFLOW CANDIDATE LINES

In step 1, the DSO determines a set of risky buses,  $\mathcal{N}_{rsk}^s$ , and a set of risky lines,  $\mathcal{L}_{rsk}^s$ . The risky buses and risky lines are candidates for overvoltage buses and overflow lines, respectively. To select the buses and the lines, power flow analysis is conducted using load forecast  $\bar{\mathbf{P}}_d$  and  $\bar{\mathbf{Q}}_d$  and DERA bids  $p_g^s$  and  $q_g^s$ , satisfying the following equations (5a–5h):

$$\theta_1^s = 0, \quad |v_1^s| = 1 \quad (5a)$$

$$p_i^s = |v_i^s| \sum_{j \in \mathcal{N}} |V_j^s| (G_{ij} \cos \theta_{ij}^s + B_{ij} \sin \theta_{ij}^s), \quad \forall i \in \mathcal{N} \quad (5b)$$

$$q_i^s = |v_i^s| \sum_{j \in \mathcal{N}} |V_j^s| (G_{ij} \sin \theta_{ij}^s - B_{ij} \cos \theta_{ij}^s), \quad \forall i \in \mathcal{N} \quad (5c)$$

$$p_i^s = p_{g,i}^s - \bar{P}_{d,i}, \quad \forall i \in \mathcal{N} \quad (5d)$$

$$q_i^s = q_{g,i}^s - \bar{Q}_{d,i}, \quad \forall i \in \mathcal{N} \quad (5e)$$

$$\begin{aligned} p_{f,l}^s &= |v_i^s| |v_j^s| (G_{ij} \cos \theta_{ij}^s + B_{ij} \sin \theta_{ij}^s) \\ &\quad - G_{ij} |V_i^s|^2, \quad \forall (i, j) = \forall l \in \mathcal{L} \end{aligned} \quad (5f)$$

$$\begin{aligned} q_{f,l}^s &= |v_i^s| |v_j^s| (G_{ij} \sin \theta_{ij}^s - B_{ij} \cos \theta_{ij}^s) \\ &\quad + B_{ij} |V_i^s|^2, \quad \forall (i, j) = \forall l \in \mathcal{L} \end{aligned} \quad (5g)$$

$$|s_{f,l}^s|^2 = \{p_{f,l}^s\}^2 + \{q_{f,l}^s\}^2, \quad \forall (i, j) = \forall l \in \mathcal{L} \quad (5h)$$

where  $\mathcal{X}_{PF}^s = \{\theta^s, |v^s|, p^s, q^s, p_f^s, q_f^s, s_f^s\}$  are the decision variables of the power flow analysis;  $G_{ij}$  and  $B_{ij}$  are the

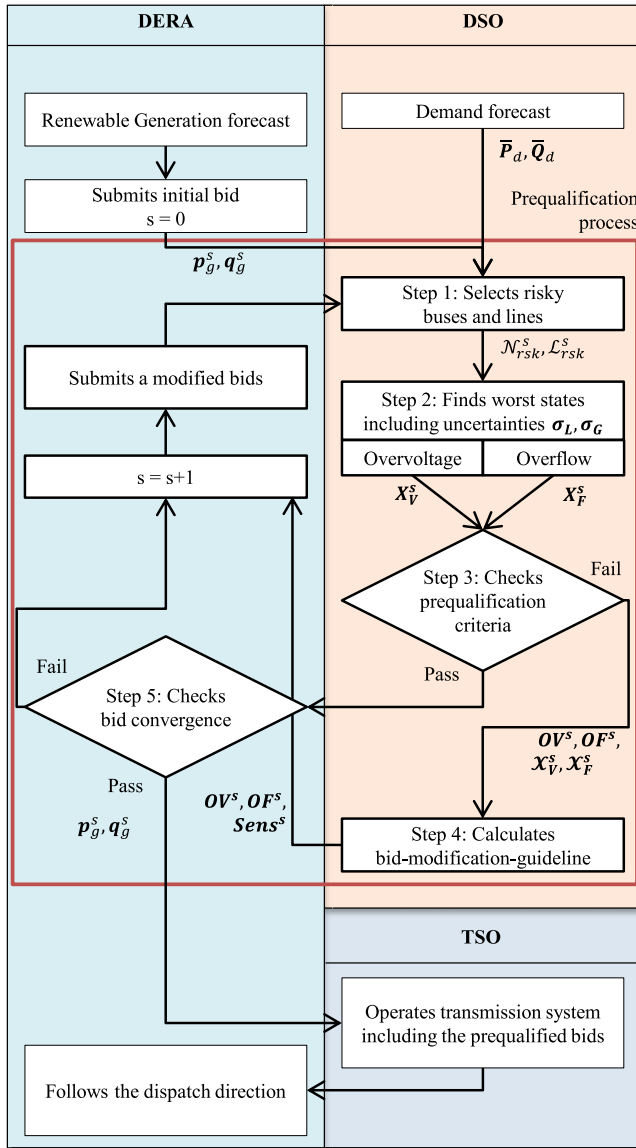


FIGURE 3. Flow chart of the prequalification process when the DSO guides the DERA bid.

conductance and susceptance, respectively;  $p_i$  and  $q_i$  are the active and reactive injected powers, respectively;  $|v_i|$  and  $\theta_i$  are the magnitude and angle of voltage, respectively;  $\theta_{ij} = \theta_i - \theta_j$ ; and  $p_{f,l}$ ,  $q_{f,l}$ , and  $s_{f,l}$  are the active, reactive, and complex power flow, respectively.

Using the result of the power flow analysis, a set of risky buses,  $\mathcal{N}_{rsk}^s$ , and a set of risky lines,  $\mathcal{L}_{rsk}^s$ , are composed in eq. (6) as follows:

$$\mathcal{N}_{rsk}^s = \left\{ b_{rsk}^{\tilde{s}} \mid b_{rsk}^{\tilde{s}} = \arg \max_{b \in \mathcal{N}} \left( |v_b^{\tilde{s}}| - \bar{V} \right), \right. \\ \left. |v_b^{\tilde{s}}| \in \mathcal{X}_{PF}^{\tilde{s}}, \forall \tilde{s} \leq s \right\} \quad (6a)$$

$$\mathcal{L}_{rsk}^s = \left\{ l_{rsk}^{\tilde{s}} \mid l_{rsk}^{\tilde{s}} = \arg \max_{l \in \mathcal{L}} \frac{|s_{f,l}^{\tilde{s}}| - \bar{S}_{f,l}}{\bar{S}_{f,l}}, \right. \\ \left. s_{f,l}^{\tilde{s}} \in \mathcal{X}_{PF}^{\tilde{s}}, \forall \tilde{s} \leq s \right\} \quad (6b)$$

where  $b_{rsk}^{\tilde{s}}$  is the overvoltage candidate bus,  $\bar{V}$  is the upper limit for the voltage magnitude,  $|v_b^{\tilde{s}}|$  is the voltage magnitude of bus  $b$ ,  $l_{rsk}^{\tilde{s}}$  is the overflow candidate line,  $\bar{S}_{f,l}$  is the capacity of line  $l$ , and  $s_{f,l}$  is the complex power flow in line  $l$ . The superscript  $\tilde{s}$  denotes each iteration that is less than or equal to  $s$ .  $\mathcal{N}_{rsk}^s$  is a set of  $b_{rsk}^{\tilde{s}}$ , where a voltage violation is the largest for each  $\tilde{s}$  (6a). Likewise,  $\mathcal{L}_{rsk}^s$  is a set of  $l_{rsk}^{\tilde{s}}$ , where a flow violation ratio is the largest for each  $\tilde{s}$  (6b).

$\mathcal{N}_{rsk}^s$  and  $\mathcal{L}_{rsk}^s$  store  $b_{rsk}^{\tilde{s}}$  and  $l_{rsk}^{\tilde{s}}$ , respectively for each  $\tilde{s}$  to prevent recurrence of the problems. If the old  $b_{rsk}^{\tilde{s}}$  and  $l_{rsk}^{\tilde{s}}$  are forgotten and only the newest  $b_{rsk}^{\tilde{s}}$  and  $l_{rsk}^{\tilde{s}}$  are managed, the previously solved problems could recur as iteration progresses. Thus, the risky buses and lines for each iteration  $s$  need to be gathered in  $\mathcal{N}_{rsk}^s$  and  $\mathcal{L}_{rsk}^s$ , respectively.  $\mathcal{N}_{rsk}^s$  and  $\mathcal{L}_{rsk}^s$  are passed to step 2 to find the worst cases of overvoltage and overflow, respectively.

## B. STEP 2: SEARCHING FOR THE WORST CASE OF THE DISTRIBUTION SYSTEM INCLUDING UNCERTAINTIES

### 1) MODELING OF UNCERTAINTY RANGES

Uncertainties of the demand forecast and the DERA bid in each bus are modeled using a pair of upper and lower boundaries. From historical data comparing metered and forecast values, the probabilistic distribution of forecast error for both demand and DRES and the range of demand within a specific confidence interval can be expressed, as shown in Figure 4. The uncertainties are formulated as follows:

$$1 - \sigma_i^{low} \leq \xi_i \leq 1 + \sigma_i^{high}, \quad \forall i \in \mathcal{N}, \mathcal{G} \\ \tilde{p}_i = \bar{p}_i \cdot \xi_i, \quad \forall i \in \mathcal{N}, \mathcal{G} \\ \tilde{q}_i = \bar{q}_i \cdot \xi_i \quad \forall i \in \mathcal{N}, \mathcal{G} \quad (7)$$

where  $\xi_i$  is a bounded random variable that indicates an uncertainty ratio of the real-time demand and DRES output to the forecast values.  $\sigma_i^{low}$  and  $\sigma_i^{high}$  are the lower and upper limits of  $\xi_i$ , respectively;  $P_i$  and  $Q_i$  are the possible real-time active and reactive power, respectively;  $P_i^{fcst}$  and  $Q_i^{fcst}$  are the active and reactive power forecasts, respectively.  $\xi_i$  is used in both active power and reactive power equations, assuming constant power factors. For the demand, a constant-power ZIP model whose power factor is irrelevant to the voltage is assumed [44]. Furthermore, it is assumed that the control signal manipulating power factor in DRESs is not given for real-time uncertainties.

### 2) SEARCHING FOR THE WORST OVERVOLTAGE STATES AND THE WORST OVERFLOW STATES

In step 2, the DSO finds the worst case when overvoltage and overflow problems occur, including uncertainties  $\sigma_L$  and  $\sigma_G$ . Two worst cases are explored; one is the worst overvoltage state  $\mathcal{X}_V^s$ , and the other is the worst overflow state  $\mathcal{X}_F^s$ .

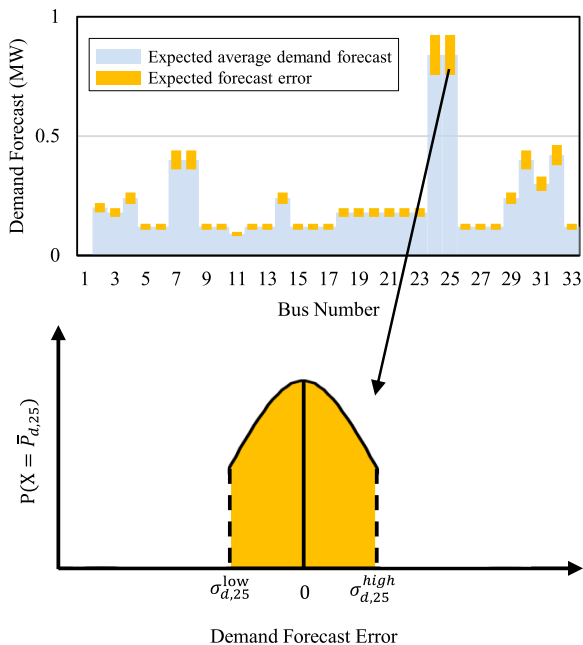


**FIGURE 4.** Example of a demand forecast and an uncertainty range for a real-time demand from the probability distribution of a forecast error as a truncated normal distribution.

*a: WORST OVERVOLTAGE STATE*

The objective function and constraints that search the worst overvoltage state  $\mathcal{X}_V^s$  are as follows:

$$\max_{\mathcal{X}_V^s} \sum_{i \in \mathcal{N}_{rsk}^s} |v_i^s| \tag{8}$$

subject to (5a–5c)

$$1 - \sigma_{g,i}^{low} \leq \xi_{g,i} \leq 1 + \sigma_{g,i}^{high}, \quad \forall i \in \mathcal{N} \tag{9a}$$

$$1 - \sigma_{d,i}^{low} \leq \xi_{d,i} \leq 1 + \sigma_{d,i}^{high}, \quad \forall i \in \mathcal{N} \tag{9b}$$

$$p_i^s = p_{g,i}^s \cdot \xi_{g,i} - \bar{P}_{d,i} \cdot \xi_{d,i}, \quad \forall i \in \mathcal{N} \tag{9c}$$

$$q_i^s = q_{g,i}^s \cdot \xi_{g,i} - \bar{Q}_{d,i} \cdot \xi_{d,i}, \quad \forall i \in \mathcal{N} \tag{9d}$$

where  $\mathcal{X}_V^s = \{\theta^s, |v^s|, \xi^s, p^s, q^s\}$  is the decision variable set of the worst overvoltage. The objective function is the sum of voltages on risky buses (8).  $\xi_{d,i}^s$  and  $\xi_{g,i}^s$  are between the upper and lower limits on each bus (9a, 9b). (9c, 9d) are equations for the active and reactive power balance that include uncertainty variables. The set of decision variables,  $\mathcal{X}_V^s$ , is passed to step 4.

*b: WORST OVERFLOW STATE*

The objective function and constraints that search the worst overflow state  $\mathcal{X}_F^s$  are as follows:

$$\max_{\mathcal{X}_F^s} \sum_{l \in \mathcal{L}_{rsk}^s} |s_{f,l}^s|^2 / |\bar{S}_{f,l}^s|^2$$

subject to (5a–5c), (5f–5h), (9a–9d) (10)

where the set of decision variables is  $\mathcal{X}_F^s = \{\theta^s, |v^s|, p^s, q^s, p_f^s, q_f^s, s_f^s\}$ . The objective function is the sum of the square line usage rates of the lines in  $\mathcal{L}_{rsk}^s$  (10). Eqs. (5a–5c) and

(9a–9d) are also included like in the worst overvoltage state. Eq. (5f–5h) are added. The results,  $\mathcal{X}_V^s$  and  $\mathcal{X}_F^s$ , are passed to step 3.

**C. STEP 3: CHECKING VIOLATIONS IN THE WORST CASE SCENARIO**

From step 2, the worst cases,  $\mathcal{X}_V^s$  and  $\mathcal{X}_F^s$ , are obtained. In step 3, the DSO checks for overvoltage problems in  $\mathcal{X}_V^s$  and overflow problems in  $\mathcal{X}_F^s$ . Overvoltage violations  $OV_i^s$  are calculated using values in  $\mathcal{X}_V^s$ , and overflow violations  $OF_l^s$  are calculated using values in  $\mathcal{X}_F^s$ .  $OV_i^s$  and  $OF_l^s$  are calculated as follows:

$$OV_i^s = |v_i^s| - \bar{V} \quad \forall i \in \mathcal{N}, \quad |V_i^s| \in |V^s| \in \mathcal{X}_V^s, \tag{11a}$$

$$OF_l^s = |s_{f,l}^s|^2 - \bar{S}_{f,l}^2 \quad \forall l \in \mathcal{L}, \quad |S_{f,l}^s| \in |S_f^s| \in \mathcal{X}_F^s, \tag{11b}$$

Each  $OV_i^s$  and  $OF_l^s$  is positive if the overvoltage or overflow occurs on each bus or line. The following conditions for  $OV^s$  and  $OF^s$  determine whether the latest DERA bid passes the prequalification process (12).

$$\max_{i \in \mathcal{N}} OV_i^s < \epsilon_V \tag{12a}$$

$$\max_{l \in \mathcal{L}} OF_l^s < \epsilon_F \tag{12b}$$

where  $\epsilon_V$  and  $\epsilon_F$  are small positive numbers that are the criteria for the prequalification test. If all  $OV^s$  and  $OF^s$  are negative, it is assumed that no problems occur even when uncertainties are realized. However, because of non-linearity of the distribution system, the bid cannot pass the prequalification process even though the DERA follows the bid-modification guidelines. Therefore, to admit trivial errors,  $\epsilon_V$  and  $\epsilon_F$  are introduced, which are set to 1.0e-4. If the conditions in (12) are satisfied, the DSO estimates its system as reliable. The prequalification process then passes to step 5. However, if the conditions in (12) are not satisfied, the system, including the uncertainties, is assumed to be unreliable, and the process passes to step 4.

**D. STEP 4: CALCULATING THE BID-MODIFICATION GUIDELINES**

In step 4, the DSO calculates the bid-modification guidelines using  $\mathcal{X}_V^s$  and  $\mathcal{X}_F^s$ . A bid-modification guideline consists of the degree of violation and sensitivity. The degree of violations is  $OV^s$  and  $OF^s$ , as determined in step 3. The methods for calculating the sensitivity are described in the following subsections.

1) VOLTAGE SENSITIVITIES

The DSO calculates the voltage sensitivity to the DERA bid based on the inverse linearized Jacobian matrix:

$$\begin{aligned} \begin{bmatrix} \Delta \theta_{-1} \\ \Delta |v_{-1}| \end{bmatrix} &= \begin{bmatrix} J_{p\theta}(x) & J_{p|v|}(x) \\ J_{q\theta}(x) & J_{q|v|}(x) \end{bmatrix}^{-1} \Big|_{x=\mathcal{X}_V^s} \begin{bmatrix} \Delta p_{-1} \\ \Delta q_{-1} \end{bmatrix} \\ &= \begin{bmatrix} Sens_{p\theta}(x) & Sens_{p|v|}(x) \\ Sens_{q\theta}(x) & Sens_{q|v|}(x) \end{bmatrix} \begin{bmatrix} \Delta p_{-1} \\ \Delta q_{-1} \end{bmatrix} \end{aligned} \tag{13}$$



where  $\mathbf{J}$  denotes the Jacobian matrix, and  $\mathbf{J}_{AB}$  is a Jacobian matrix of  $A$  to  $B$  for  $\mathbf{J}_{p\theta}$ ,  $\mathbf{J}_{p|v|}$ ,  $\mathbf{J}_{q\theta}$ , and  $\mathbf{J}_{q|v|}$ ;  $\Delta\theta_{-1} = [\Delta\theta_2, \dots, \Delta\theta_{\mathcal{N}}]$ ,  $\Delta|v_{-1}| = [\Delta|v_2|, \dots, \Delta|v_{\mathcal{N}}|]$ ,  $\Delta\mathbf{p}_{-1} = [\Delta p_2, \dots, \Delta p_{\mathcal{N}}]$ , and  $\Delta\mathbf{q}_{-1} = [\Delta q_2, \dots, \Delta q_{\mathcal{N}}]$ , are small variations in the voltage angle, voltage magnitude, active power, and reactive power, respectively;  $\mathbf{Sens}_{p\theta}$  and  $\mathbf{Sens}_{q\theta}$  are the sensitivity matrices of the voltage angle to the active and reactive power, respectively;  $\mathbf{Sens}_{p|v|}$  and  $\mathbf{Sens}_{q|v|}$  are sensitivity matrices of the voltage magnitude to the active and reactive power, respectively. It should be noted that  $\mathcal{X}_V^s$  is used to calculate Jacobian matrices (13).

## 2) FLOW SENSITIVITIES

The DSO also calculates flow sensitivity to the DERA bid. The flow sensitivity is obtained using partial differentiation and the chain rule, which are calculated as follows:

$$|s_{f,l}|^2 = p_{f,l}^2 + q_{f,l}^2, \quad (14a)$$

$$\mathbf{Sens}_{sp,l,k}^s = \frac{\partial |s_{f,l}|^2}{\partial p_k} = 2 \left( p_{f,l} \frac{\partial p_{f,l}}{\partial p_k} + q_{f,l} \frac{\partial q_{f,l}}{\partial p_k} \right) \Big|_{x=\mathcal{X}_F^s}, \quad (14b)$$

$$\mathbf{Sens}_{sq,l,k}^s = \frac{\partial |s_{f,l}|^2}{\partial q_k} = 2 \left( p_{f,l} \frac{\partial p_{f,l}}{\partial q_k} + q_{f,l} \frac{\partial q_{f,l}}{\partial q_k} \right) \Big|_{x=\mathcal{X}_F^s} \quad \forall l \in \mathcal{L}, \forall k \in \mathcal{N} \quad (14c)$$

where

$$\frac{\partial p_{f,l}}{\partial p_k} = \frac{\partial p_{f,l}}{\partial |v_i|} \frac{\partial |v_i|}{\partial p_k} + \frac{\partial p_{f,l}}{\partial |v_j|} \frac{\partial |v_j|}{\partial p_k} + \frac{\partial p_{f,l}}{\partial \theta_i} \frac{\partial \theta_i}{\partial p_k} + \frac{\partial p_{f,l}}{\partial \theta_j} \frac{\partial \theta_j}{\partial p_k} \quad (14d)$$

$$\frac{\partial q_{f,l}}{\partial p_k} = \frac{\partial q_{f,l}}{\partial |v_i|} \frac{\partial |v_i|}{\partial p_k} + \frac{\partial q_{f,l}}{\partial |v_j|} \frac{\partial |v_j|}{\partial p_k} + \frac{\partial q_{f,l}}{\partial \theta_i} \frac{\partial \theta_i}{\partial p_k} + \frac{\partial q_{f,l}}{\partial \theta_j} \frac{\partial \theta_j}{\partial p_k} \quad (14e)$$

$$\frac{\partial p_{f,l}}{\partial q_k} = \frac{\partial p_{f,l}}{\partial |v_i|} \frac{\partial |v_i|}{\partial q_k} + \frac{\partial p_{f,l}}{\partial |v_j|} \frac{\partial |v_j|}{\partial q_k} + \frac{\partial p_{f,l}}{\partial \theta_i} \frac{\partial \theta_i}{\partial q_k} + \frac{\partial p_{f,l}}{\partial \theta_j} \frac{\partial \theta_j}{\partial q_k} \quad (14f)$$

$$\frac{\partial q_{f,l}}{\partial q_k} = \frac{\partial q_{f,l}}{\partial |v_i|} \frac{\partial |v_i|}{\partial q_k} + \frac{\partial q_{f,l}}{\partial |v_j|} \frac{\partial |v_j|}{\partial q_k} + \frac{\partial q_{f,l}}{\partial \theta_i} \frac{\partial \theta_i}{\partial q_k} + \frac{\partial q_{f,l}}{\partial \theta_j} \frac{\partial \theta_j}{\partial q_k} \quad (14g)$$

$$\frac{\partial p_{f,l}}{\partial |v_i|} = |v_j|(G_{ij} \cos \theta_{ij} + B_{ij} \sin \theta_{ij}) - 2G_{ij}|v_i| \quad (14h)$$

$$\frac{\partial p_{f,l}}{\partial |v_j|} = |v_i|(G_{ij} \cos \theta_{ij} + B_{ij} \sin \theta_{ij}) \quad (14i)$$

$$\frac{\partial p_{f,l}}{\partial \theta_i} = |v_i||v_j|(-G_{ij} \sin \theta_{ij} + B_{ij} \cos \theta_{ij}) \quad (14j)$$

$$\frac{\partial p_{f,l}}{\partial \theta_j} = |v_i||v_j|(G_{ij} \sin \theta_{ij} - B_{ij} \cos \theta_{ij}) \quad (14k)$$

$$\frac{\partial q_{f,l}}{\partial |v_i|} = |v_j|(G_{ij} \sin \theta_{ij} - B_{ij} \cos \theta_{ij}) + 2B_{ij}|v_i| \quad (14l)$$

$$\frac{\partial q_{f,l}}{\partial |v_j|} = |v_i|(G_{ij} \sin \theta_{ij} - B_{ij} \cos \theta_{ij}) \quad (14m)$$

$$\frac{\partial q_{f,l}}{\partial \theta_i} = |v_i||v_j|(G_{ij} \cos \theta_{ij} + B_{ij} \sin \theta_{ij}) \quad (14n)$$

$$\frac{\partial p_{f,l}}{\partial |v_i|} = |v_j|(G_{ij} \cos \theta_{ij} + B_{ij} \sin \theta_{ij}) - 2G_{ij}|v_i| \quad (14o)$$

$\mathbf{Sens}_{SP,l,k}^s$  is the sensitivity of  $|s_{f,l}|^2$  to  $p_k$ , and  $\mathbf{Sens}_{SQ,l,k}^s$  is the sensitivity of  $|s_{f,l}|^2$  to  $q_k$ . It should be noted that the values in  $\mathcal{X}_F^s$  are used to calculate the sensitivities to reflect the worst overflow state (14b, 14c).

## 3) BID-MODIFICATION GUIDELINES FOR THE DERA

After the DSO calculates  $\mathbf{OV}^s$ ,  $\mathbf{OF}^s$ ,  $\mathbf{Sens}_{vp}$ ,  $\mathbf{Sens}_{vq}$ ,  $\mathbf{Sens}_{sp}$ , and  $\mathbf{Sens}_{sq}$ , the DSO sends the bid-modification guidelines as linear constraints, which are as follows:

$$-\mathbf{OV}_i^s \geq \sum_{j \in \mathcal{G}} (\mathbf{Sens}_{vp,i,j}^s \Delta p_{g,j}^s + \mathbf{Sens}_{vq,i,j}^s \Delta q_{g,j}^s), \quad \forall i \in \mathcal{N} \quad (15a)$$

$$-\mathbf{OF}_l^s \geq \sum_{k \in \mathcal{G}} (\mathbf{Sens}_{sp,l,k}^s \Delta p_{g,k}^s + \mathbf{Sens}_{sq,l,k}^s \Delta q_{g,k}^s), \quad \forall l \in \mathcal{L} \quad (15b)$$

where the set of decision variables is  $\Delta \mathbf{p}_g^s$  and  $\Delta \mathbf{q}_g^s$ .  $\Delta \mathbf{p}_g^s$  is the modification of the active power bid, and  $\Delta \mathbf{q}_g^s$  is the modification of the reactive power bid. Eq. (15) represents the constraint in which the values of  $\mathcal{X}_V^s$  and  $\mathcal{X}_F^s$  are substituted into eq. (4). As DERA submits a modified bid satisfying eq. (15), the process goes back to step 1.

## E. STEP 5: CHECK BID CONVERGENCE

In step 5, the DERA decides whether to modify the bid again or to accept the prequalification result and submit the qualified bid to the wholesale market. As the iteration progresses, the DERA bids converge in the point that maximizes the profit of DERA without causing the overvoltage and overflow problems.

## V. CASE STUDY AND DISCUSSION

### A. SIMULATION SETTINGS

#### 1) FORMULATIONS OF DISTRIBUTED ENERGY RESOURCE AGGREGATOR

To verify the proposed prequalification process, let us consider a DERA with the following objective function and constraints. The DERA aims to maximize its profits on the energy market without considering information related to physical constraints in the distribution system. The objective function and constraints are as follows:

$$\max_{\mathcal{X}_{bid}^{s=0}} \sum_{i \in \mathcal{G}} p_{g,i}^s \quad (16)$$

$$\text{subject to } (p_{g,i}^s)^2 + (q_{g,i}^s)^2 \leq (\bar{P}_{g,i})^2, \quad \forall i \in \mathcal{G} \quad (17a)$$

$$q_{g,i}^s \leq \left| p_{g,i}^s \tan(\arccos(\underline{pf})) \right|, \quad \forall i \in \mathcal{G} \quad (17b)$$

TABLE 4. Test system parameters: line parameters.

Line $l$	Start bus	End bus	R [ohm]	$X_l$ [ohm]	$ \bar{S}_{f,l} $ [MVA]	Line $l$	Start bus	End bus	R [ohm]	$X_l$ [ohm]	$ \bar{S}_{f,l} $ [MVA]	Line $l$	Start bus	End bus	R [ohm]	$X_l$ [ohm]	$ \bar{S}_{f,l} $ [MVA]
1	1	2	0.09	0.05	7.07	12	12	13	1.47	1.16	2.24	23	23	24	0.90	0.71	2.24
2	2	3	0.49	0.25	5.48	13	13	14	0.54	0.71	2.24	24	24	25	0.90	0.70	2.24
3	3	4	0.37	0.19	3.87	14	14	15	0.59	0.53	2.24	25	6	26	0.20	0.10	2.24
4	4	5	0.38	0.19	3.87	15	15	16	0.75	0.55	2.24	26	26	27	0.28	0.14	2.24
5	5	6	0.82	0.71	3.87	16	16	17	1.29	1.72	2.24	27	27	28	1.06	0.93	2.24
6	6	7	0.19	0.62	2.24	17	17	18	0.73	0.57	2.24	28	28	29	0.80	0.70	2.24
7	7	8	0.71	0.24	2.24	18	2	19	0.16	0.16	2.24	29	29	30	0.51	0.26	2.24
8	8	9	1.03	0.74	2.24	19	19	20	1.50	1.36	2.24	30	30	31	0.97	0.96	2.24
9	9	10	1.04	0.74	2.24	20	20	21	0.41	0.48	2.24	31	31	32	0.31	0.36	2.24
10	10	11	0.20	0.07	2.24	21	21	22	0.71	0.94	2.24	32	32	33	0.34	0.53	2.24
11	11	12	0.37	0.12	2.24	22	3	23	0.45	0.31	2.24						

where the set of decision variables is  $\mathcal{X}_{bid}^{s=0} = \{p_g^0, q_g^0\}$ ;  $\mathcal{G}$  is a set of generator bus indexes;  $p_{g,i}^s$  and  $q_{g,i}^s$  are the active and reactive power of the DERA bid, respectively;  $\bar{P}_{g,i}$  is the DRES output forecast; and  $\underline{pf}$  is the lower limit of the power factor. After step 4 of the prequalification process, the DERA modifies its bid to include the bid-modification guidelines. The formulations, including the guidelines, are as follows:

$$\max_{\mathcal{X}_{bid}^s} \sum_{i \in \mathcal{G}} p_{g,i}^s \quad (18)$$

subject to (15, 17)

$$p_{g,i}^s = p_{g,i}^{s-1} + \Delta p_{g,i}^s, \forall i \in \mathcal{G} \quad (19a)$$

$$q_{g,i}^s = q_{g,i}^{s-1} + \Delta q_{g,i}^s, \forall i \in \mathcal{G} \quad (19b)$$

where the set of decision variables is  $\mathcal{X}_{bid}^s = \{R_E^s, p_g^s, q_g^s, \Delta p_g^s, \Delta q_g^s\}$ ;  $\Delta p_g^{bid,s}$  and  $\Delta q_g^{bid,s}$  are the modifications in the active and reactive power bid, respectively. The objective function and constraints in the initial bidding are also included. The DERA relieves violations of  $OV^s$  and  $OF^s$  by modifying  $\Delta p_g^{bid,s}$  and  $\Delta q_g^{bid,s}$ , respectively (19a, 19b). The DERA submits updated values of  $p_g^s$  and  $q_g^s$  to the DSO, and the next iteration begins from step 1 all over again.

Although the DSO was not meant to do this, it can unintentionally suppress the DERA bid because of the nonlinearity of the distribution system. Although the bid is prequalified, the DERA can increase its output in the system constraints.

Therefore, even though the bid is prequalified, the DERA could be dissatisfied with its bid. To resolve this situation, the proposed algorithm allows the DERA to decide whether to submit a prequalified bid to the TSO or return to the prequalification process. It is assumed that the DERA decides based on the following criterion (20):

$$\left| \sum_{i \in \mathcal{G}} \{p_{g,i}^s - p_{g,i}^{s-1}\} \right| \leq \epsilon_B \quad (20)$$

where  $\epsilon_B$  is a positive small number. When the sum of the DRES outputs converges, the DRES generation can no longer be increased in the distribution system. Therefore, the convergence of the sum of the DRES outputs is set as the convergence criterion. If the criterion is satisfied, then the

DERA is satisfied with its qualified bid and submits the bid to the wholesale market. Subsequently, the prequalification process is terminated.

## 2) PARAMETERS

The proposed prequalification algorithm is verified using the IEEE33-bus distribution system in [45] and presented in Figure 5. Bus 1 is the slack bus, representing the interconnection point with the transmission system. The line parameters are taken from [45] and are listed in Table 4.

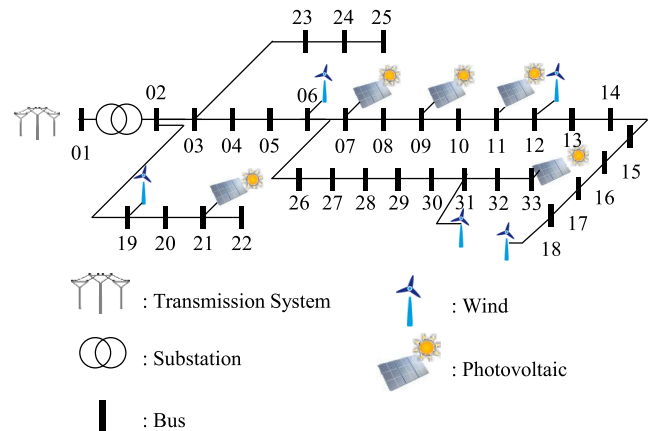


FIGURE 5. IEEE 33-bus distribution network with a high penetration of distributed renewable energy sources.

The demand and generation are presented in Table 5. To increase the line usage rate, which is a severe situation in the distribution system, the active power demand in each bus is set to twice the original data given in [45], whereas the reactive power demand is set to be equal to that in [45]. Five wind generators are assumed to be located in buses 6, 12, 31, 18, and 19, and five photovoltaic generators are located in buses 7, 9, 11, 33, and 21. To assume a distribution system with a large integration of DRESs, the output of the wind and photovoltaic generators are doubled compared to the original data [46]. The total amounts of active power demand, reactive power demand, and generation are set to 7.43, 2.30, and 12.00, respectively.

TABLE 5. Test system parameters: Load and generation parameters.

Bus $i$	$\bar{P}_{d,i}$ [MW]	$\bar{Q}_{d,i}$ [MW]	$\bar{P}_{g,i}$ [MW]	Bus $i$	$\bar{P}_{d,i}$ [MW]	$\bar{Q}_{d,i}$ [MW]	$\bar{P}_{g,i}$ [MW]
1	-	-	-	18	0.18	0.04	1.2
2	0.2	0.06	-	19	0.18	0.04	1.92
3	0.18	0.04	-	20	0.18	0.04	-
4	0.24	0.08	-	21	0.18	0.04	0.54
5	0.12	0.03	-	22	0.18	0.04	-
6	0.12	0.02	2.4	23	0.18	0.05	-
7	0.4	0.1	0.36	24	0.84	0.2	-
8	0.4	0.1	-	25	0.84	0.2	-
9	0.12	0.02	0.54	26	0.12	0.025	-
10	0.12	0.02	-	27	0.12	0.025	-
11	0.09	0.03	0.54	28	0.12	0.02	-
12	0.12	0.035	1.2	29	0.24	0.07	-
13	0.12	0.035	-	30	0.4	0.6	-
14	0.24	0.08	-	31	0.3	0.07	2.4
15	0.12	0.01	-	32	0.42	0.1	-
16	0.12	0.02	-	33	0.12	0.04	0.9
17	0.12	0.02	-	Sum	7.43	2.3	12

Three cases are simulated to demonstrate the robustness of the proposed prequalification scheme. Inspired by [39], Case I conducts a prequalification only to relieve overflow problems and ignore the uncertainties. Case II is an improved model based on Case I, in which the DSO considers uncertainties from its system, but the voltage constraint is still not considered. Case III prevents both overvoltage and overflow problems by considering uncertainties.

Parameters of the three cases are provided in Table 6. To consider the voltage constraint, the upper limit of the voltage magnitude is set only in Case III. To ignore uncertainties, the ranges of the DERA bid and demand are set to zero in Case I, whereas each uncertainty range is set to 10 % in Cases II and III. All other parameters are set to the same value in the three cases.

The unit of voltage magnitude is per unit of which base voltage is 12.66 kV. The line usage rate in percentage [%] on each line is  $|s_{f,l}|$  divided by  $|\bar{S}_l|$ .

The simulations are conducted under the Julia/JuMP environment using the IPOPT solver to solve the non-linear programming problem. The tolerance is set to  $1e-7$  for all simulations. An Intel Core i7-8656U CPU @ 1.80 GHz is used to run the simulations.

**B. COMPARISON OF THE PROPOSED METHOD AND THE BRUTE-FORCE SEARCH METHOD**

The brute-force search method finds  $nb$  scenarios in which the bus voltage is maximum and  $nl$  scenarios in which the line usage rate is maximum in each line. In contrast, the proposed method finds only two scenarios wherein the sum of the bus voltages in  $\mathcal{N}_{rsk}$  is maximum and the sum of the line usage rates in the lines in  $\mathcal{L}_{rsk}$  is the maximum.

Table 7 presents a comparison of the two methods. Because the brute-force search method finds  $nb + nl$  uncertainty scenarios, it takes a longer time for the DSO to review the system compared to the proposed method. The proposed method

TABLE 6. Test system parameters: uncertainty range, constraint inputs, and convergence criteria.

Parameters	Case		
	I [39]	II	III
Upper and lower range of $\xi_g; \sigma_g^l, \sigma_g^h$	0	10 %	10 %
Upper and lower range of $\xi_d; \sigma_d^l, \sigma_d^h$	0	10 %	10 %
Voltage upper limit $\bar{V}$	-	-	1.05
DRES power factor limit $pf$	1	1	1
$\epsilon_V, \epsilon_F, \epsilon_B$	1.0E-3	1.0E-3	1.0E-3

TABLE 7. The ratio of overvoltage violation and overflow violation among all scenarios.

	Proposed method	Brute-force search method
Number of risky scenario	2	$nb + nl$
Number of guidelines transferred from DSO to DERA	$nb + nl$	$nb^2 + nl^2$
Running time (sec)	18.68	233.01
Sum of DRES outputs (MW)	9.244	9.240

requires 18.68 s only, which is much less than the 233.01 s required for the brute-force search method.

Furthermore, the DSO transfers  $nb^2 + nl^2$  constraints to the DERA in the brute-force search method. However, the constraints decrease to only  $nb + nl$  in the proposed method. Moreover, the sum of the DRESs' output only differs by 0.04 % in both methods. The result demonstrates that the proposed method enables the DSO to review DERA's bid in a more efficient manner.

**C. EFFECT OF UNCERTAINTY ON THE OVERVOLTAGE AND OVERFLOW**

To confirm the impact of uncertainties, Figure 6 depicts the state of the bus voltages and line flows in both cases, with

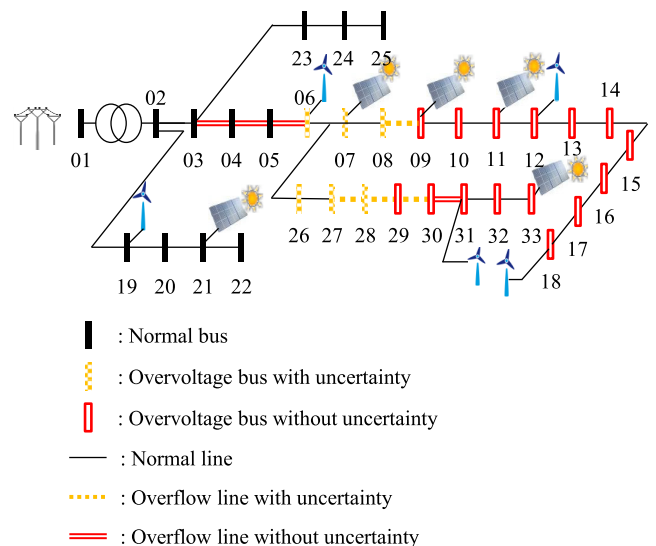


FIGURE 6. Overvoltage buses and overcurrent lines in the first iteration of Cases I, II, and III.

and without the uncertainties. The pattern of each bus and line represents one of the following states: 1) Black state: no problem occurs even though uncertainties are included. 2) Yellow state: a problem occurs when uncertainties are included. 3) Red state: a problem occurs regardless of the inclusion of uncertainties.

In Case I, the DSO restrains problems that would occur in the red lines while ignoring uncertainties. In Case II, the DSO prevents expected problems that could occur in the yellow and red lines considering the uncertainties. In Case III, the DSO prevents expected overvoltage and overflow problems that could occur in the yellow and red buses and lines considering uncertainties.

**D. COMPARISON OF THE RESULTS FOR EACH CASE UNDER UNCERTAINTY SCENARIOS**

A Monte Carlo based simulation is conducted to verify the robustness of the proposed prequalification scheme. To represent a real-time situation, 100,000 test scenarios with forecast errors are generated. Furthermore, to determine the errors of the DRES schedules and demand forecasts, each scenario has 42 random variables, including 10 random variables for each DRES and 32 random variables for the demand on each bus. Each random variable is distributed with a truncated normal distribution  $T(0, 0.061^2, [-0.1, 0.1])$ , of which the lower and upper limits are -0.1 and 0.1, respectively. In each scenario, the violations of the voltage and flow constraints are evaluated. By calculating the power flow using the generated scenarios with forecast errors, the voltage magnitude in each bus and flow in each line are calculated for each scenario. The maximum voltage and maximum line usage rate in each scenario are obtained from the calculated voltage magnitudes and flows, respectively.

Figure 7 illustrates the distribution of the maximum voltage and maximum line usage rate for each scenario, where each dot represents an individual scenario in Cases I, II, and III. The vertical dashed line denotes the upper limit of the voltage. The dots on the right side of the line indicate that the voltage constraint is violated in those scenarios. The horizontal dashed line denotes the upper limit of the line usage rate. The dots above this line indicate that the flow constraint is violated in those scenarios. The ratio of the overvoltage and overflow scenarios in each case is presented in Table 8.

In Case I, it is demonstrated that all the scenarios (100.00%) violate the voltage constraints, and the overflow problem occurs in 61.11 % of scenarios. The reason for such a high rate is that Case I did not consider the impact of the uncertainties in the prequalification process. In Case II, overvoltage still occurs in 81.12 % of the scenarios. However, no scenario experiences an overflow because Case II manages congestion by considering the influence of uncertainties. Furthermore, no overvoltage and overflow occur in Case III. The results demonstrate that the proposed prequalification algorithm works in the intended way and enables the DSO to manage anticipated threats from uncertainties. It is demonstrated that the ratio of overvoltage scenarios in

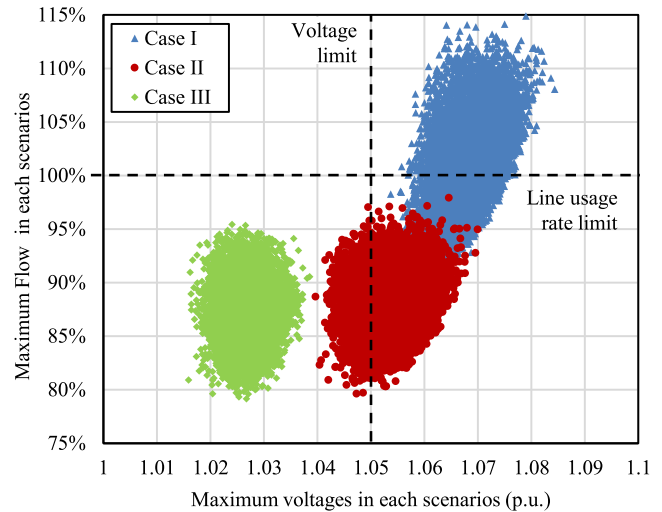


**FIGURE 7. Maximum voltage and line usage rates for each case in each uncertainty scenario.**

**TABLE 8. The ratio of overvoltage violation and overflow violation among all scenarios.**

	The ratio of scenarios	
	overvoltage	overflow
Case I	100%	60.24%
Case II	81.60%	0.00%
Case III	0.00%	0.00%

Case II is 81.60 %, which is smaller than the 100% ratio in Case I, even though Case II did not manage the overvoltage problems. The reason for this is that the some overvoltage problems are mitigated when the DRES output is reduced to prevent overflow problems. Additionally, in Case III, there is no scenario where the maximum flow exceeds the flow limit. Figure 7 shows that the distribution in Case III does not breach the line usage rate and voltage limits. The reasons for this trend will be presented in Figures 8 and 9.

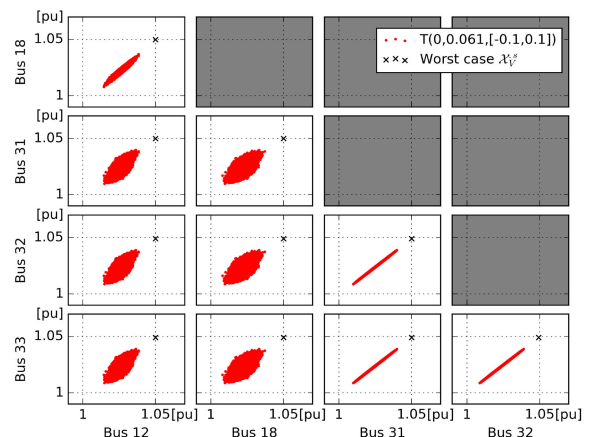


**FIGURE 8. Voltage distributions on buses 12, 18, 31, 32, and 33.**

Figure 8 presents the voltage distribution between two buses among the five buses, namely buses 12, 18, 31, 32,

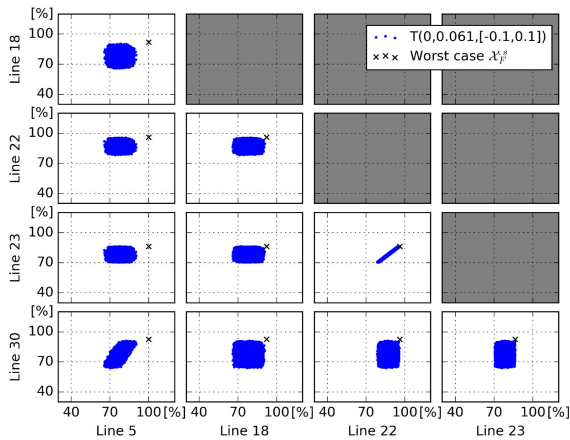


FIGURE 9. Distribution of line usage rates on lines 5, 18, 22, 23, and 30.

and 33, in Case III. Table 9 presents the Pearson correlation coefficient between the bus voltages. The five buses exhibit a high average voltage in the Monte Carlo scenarios. The figure shows that the voltage distribution between buses 12 and 18 and the distribution among buses 31, 32, and 33 are highly correlated. The reason can be that buses 12 and 18 are on the same main feeder, and buses 31, 32, and 33 are adjacent buses. Other distributions also exhibit a high positive correlation, even though no two buses are adjacent. It is shown that the worst case found by the proposed method reached a voltage limit of 1.05 p.u., but the Monte Carlo distribution did not. This indicates that the proposed method can find the worst case, which is difficult to find in the Monte Carlo method. This confirms that the worst scenario that maximizes the sum of risky bus voltages is represented by the points where each risky bus has the maximum voltage.

Figure 9 presents the distribution of the line usage rates between two lines among the five lines, namely lines 5, 18, 22, 23, and 30, in Case III. On average, the five lines have a high usage rate in the scenarios of Case III. Table 10 presents the Pearson correlation coefficient between the line usage rates. The correlation coefficient between lines 22 and 23 is 0.989. It can be inferred that they are highly correlated because both lines are adjacent. The correlation coefficient between lines 5 and 30 also exhibits a positive value of 0.745. It is demonstrated that the other lines are independent of each other. Although there are no correlations, the distributions are rectangular. In each distribution, black circle point represents scenario when the sum of the line usage rate for both lines is the biggest. Simultaneously, this point has a bigger value on both axes than most points in the distribution. Some points have a bigger value than the black circle point in the distribution because the distributions are not perfect rectangles. However, the proposed method found the worst case, which is marked as x. The worst case has bigger values than other points in the distribution. Furthermore, the point is where the sum of the line usage rate for both lines is maximized. This confirms that the worst scenario, which maximizes the sum

TABLE 9. Pearson correlation coefficient between bus voltages.

Bus #	Bus #			
	12	18	31	32
18	0.965	-	-	-
31	0.706	0.636	-	-
32	0.705	0.635	1.000	-
33	0.705	0.635	1.000	1.000

TABLE 10. Pearson correlation coefficient between line usage rates.

Line #	Line #			
	5	18	22	23
18	0.003	-	-	-
22	0.006	0.003	-	-
23	0.006	0.004	0.989	-
30	0.745	0.002	0.005	0.005

of the line usage rates for the risky lines, is the point where each risky line has the maximum line usage rate.

Figure 10 shows the trend in the ratios of the overvoltage and overflow scenarios using standard deviation of the random variable in Case III. In particular, to evaluate the robustness of the proposed method, a normal distribution with no upper and lower limits is used. In the figure,  $P(-0.1 < X < 0.1)$  denotes a probability that a random variable lies between  $-0.1$  and  $0.1$ , which is the uncertainty range covered in the prequalification process in Case III. Even though the standard deviation increases, the range covered by the prequalification remains close to 100% in the *overestimate interval*. It is shown that the ratios of the overvoltage and overflow scenarios are close to 0%. In the *robust interval*, the ratios still do not increase, even though the range covered by the prequalification decreases to 85%. In the *underestimate interval*, as the standard deviation increases, the ratio of the overflow and overvoltage scenarios starts to increase. This is because the scenarios that are worse than the expected worst case in the prequalification become more frequent.

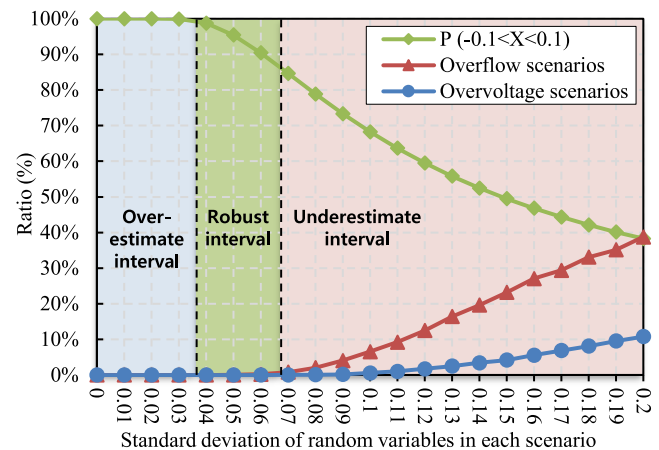


FIGURE 10. Ratio of the overvoltage and overflow scenarios.

TABLE 11. Detailed results of the prequalification process in Case III.

	Iteration $s$				
	0	1	2	3	4
Maximum voltage in $\mathcal{X}_V^s$ (Bus #)	1.1191(18)	1.0411(31)	1.0507(33)	1.0499(12)	1.0500(33)
Overvoltage buses in $\mathcal{X}_V^s$	6-18, 26-33	-	12, 31-33	-	-
Maximum overvoltage violation in $\mathcal{X}_V^s$	0.069	<b>-0.009</b>	7.4e-04	<b>-6.2e-05</b>	<b>7.5e-06</b>
Maximum line usage rate in $\mathcal{X}_F^s$ [%] (Line #)	288.05 (5)	122.70 (5)	98.70 (5)	100.13 (5)	99.99 (5)
Overflow lines in $\mathcal{X}_F^s$	3-5, 8, 27-30	4, 5	-	5	-
Maximum overflow violation in $\mathcal{X}_F^s$ [%]	188.05	22.70	<b>-1.30</b>	0.13	<b>-0.01</b>
Prequalification result of DERA bid	Not qualified	Not qualified	Not Qualified	Not Qualified	<b>Qualified</b>
Sum of the DRES output in DERA bids	12.00	9.45	9.22	9.24	9.24
Difference between the sum of the DRES outputs	-	2.55	0.23	-0.02	<b>0.00</b>
Whether the DERA bid converged or not	-	No	No	No	<b>Yes</b>

The results indicate that it is imperative for the DSO to set the uncertainty range properly before the prequalification process. When the DSO overestimates the uncertainties, there can a side effect in that the DSO can excessively decrease the profit of the DERA. Further study regarding the effect of the uncertainty range on the DERA profit is provided in Section V-F. In contrast, if the DSO underestimates the risk and sets the uncertainty range to be smaller than the real value, the risk of overvoltage or overflow problems increases.

**E. DETAILED RESULT FOR THE PROPOSED ALGORITHM IN CASE III**

Figure 11 and Tables 11 and 12 present the detailed results for Case III from iterations  $s = 0$  to  $s = 4$ . Figure 11-(a) presents the voltage profiles on the selected buses in  $\mathcal{X}_V^s$ . Figure 11-(b) presents the line usage rates on the selected lines in  $\mathcal{X}_F^s$ . Table 12 presents the DERA bid in each iteration. In iteration  $s = 0$ , the overvoltage problem occurs on buses 6 to 18 and buses 26 to 33. The maximum voltage is 1.1191 p.u. on bus 18. Moreover, the overflow problem occurs in lines 3 to 5, line 8, and lines 27 to 30. The maximum line usage rate is 288.05 % on line 5.

TABLE 12. Result of DERA bid in each step in Case III.

Bus $i$	$P_{g,i}^s$				
	$s=0$	$s=1$	$s=2$	$s=3$	$s=4$
6	2.40	2.40	1.34	1.44	1.43
7	0.36	0.36	0	0	0
9	0.54	0.54	0.54	0.54	0.54
11	0.54	0.54	0.54	0.54	0.54
12	1.20	0.68	1.20	1.15	1.16
18	1.20	0.42	0.53	0.53	0.53
19	1.92	1.92	1.92	1.92	1.92
21	0.54	0.54	0.54	0.54	0.54
31	2.40	1.78	2.40	2.40	2.40
33	0.90	0.27	0.21	0.18	0.18
sum	12.00	9.45	9.22	9.24	9.24
difference	-	2.55	0.23	-0.02	0.00

In iteration  $s = 1$ , to mitigate the overvoltage and overflow problems, the DERA reduces the sum of the DRES outputs from 12.00 MW to 9.45 MW. Even though the sum

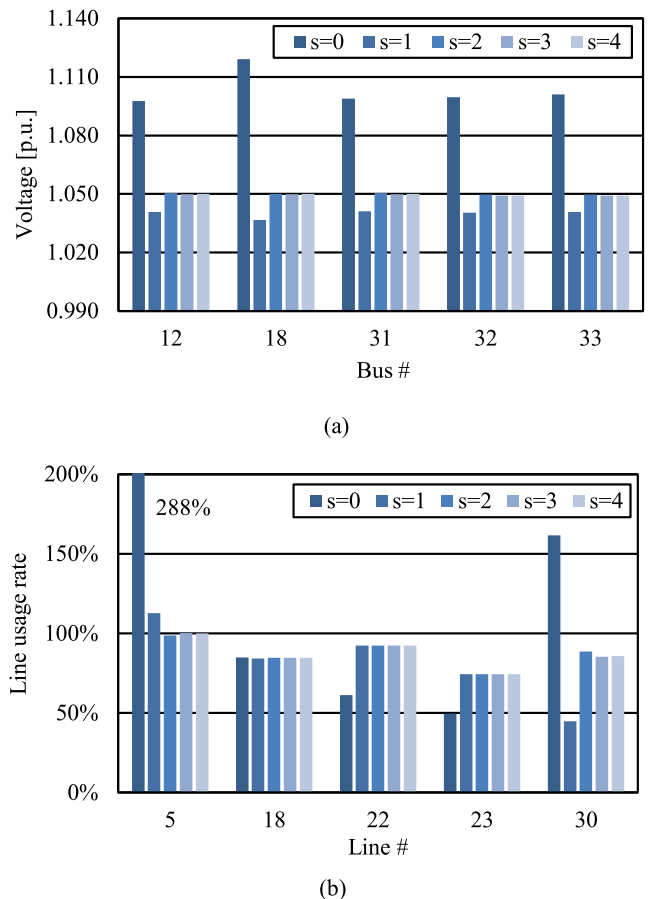


FIGURE 11. Comparison of the system states for iterations  $s = 0$  to  $s = 3$  in step 3 under Case III: (a) Voltage profiles in  $\mathcal{X}_V^s$ ; (b) Line usage rates in  $\mathcal{X}_F^s$ .

is decreased, the outputs of the DRESs on bus 9, 11, 19, and 21 do not decrease. Specifically, the DRES outputs on buses 19 and 21 are not modified because those DRESs are far from the overvoltage buses. As a result, all overvoltage problems are mitigated, and the maximum voltage decreases to 1.0411, which is lower than the voltage limit of 1.05 p.u. However, overflow problems still exist in lines 4 and 5.

Thus, the DERA reduces the sum of DRES outputs once again to mitigate the remaining overflow problem in line 5 of iteration  $s = 2$ . The outputs of DRESs on buses 6, 7, 31,

and 33 are decreased, and those on buses 12, 18, and 31 are increased. It can be inferred that sensitivities to the flow of line 5 are greater in buses 6, 7, 31, and 33 than in buses 12, 18, and 31. Owing to the decrease in the sum of DRES outputs, the overflow problem is mitigated but an overvoltage problem with a small violation recurs. Although the DERA follows the guidelines from the DSO, an unintended violation occurs because of non-linearity of the distribution system. Thus, the process progresses to the next iteration.

Despite an increase in the sum of the DRESs output, the small overvoltage violation is resolved, but a small overflow violation occurs in iteration  $s = 3$ . It can be inferred that the DERA resolved the overvoltage problem in bus 33 by decreasing the DRES output that is more sensitive and increased the output of bus 12, which is insensitive to the voltage of bus 33.

In iteration  $s = 4$ , because the DERA bid is qualified and the bid convergence criterion is also satisfied, the prequalification process is terminated. The results demonstrate that most overvoltage and overflow problems are resolved in iteration  $s = 1$  or  $s = 2$ . Furthermore, small violations and bid convergence conditions cause an increase in the number of iterations of the process. It can be inferred that the additional safety margin for the voltage limit and line usage rates can reduce the number of iterations.

**F. EFFECT OF THE EVALUATED UNCERTAINTY RANGE ON THE DERA PROFIT**

To evaluate the impact of the DSO’s uncertainty assessment on the profit of DERA, the profits under various uncertainty ranges are compared.  $\sigma_{g,i}^{low}$  and  $\sigma_{g,i}^{high}$  are assumed to be the same values, and  $\sigma_{d,i}^{low}$  and  $\sigma_{d,i}^{high}$  are also assumed to be the same values. The DERA profits in the simulation sets are compared across 121 parameter sets as  $\sigma_{g,i}^{low}$  and  $\sigma_{g,i}^{high}$  range from 0 % to 10 %, and  $\sigma_{d,i}^{low}$  and  $\sigma_{d,i}^{high}$  range from 0 % to 10 %.

To compare the DERA profits for each set of parameters, the relative profits are used. The relative profit is the value expressed as a ratio of each profit to the total profit when  $\sigma_{g,i}^{low}$ ,  $\sigma_{g,i}^{high}$ ,  $\sigma_{d,i}^{low}$ , and  $\sigma_{d,i}^{high}$  are 10 %.

The result is given in Figure 12. The brightness of each cell denotes a relative profit for the DERA. The darker the cell, the closer the relative profit is to 1.15, and the brighter the cell, the closer the relative profit is to 1. When the uncertainty range of demands is fixed, a bigger uncertainty of the DRESs leads to a smaller profit of the DERA.

To compare the impacts of the uncertainty range of a single DRES, the simulations are conducted where the conditions are nearly the same as Case III in Table 6 and only an uncertainty range of one DRES is changed. Four DRESs are selected based on the following conditions from Figure 6: the DRES on bus 18, 6, 31 and 19. The results are shown in Figure 13. Regarding the DRESs on bus 6, 18, and 31, the smaller uncertainty ranges  $\sigma_{g,6}$ ,  $\sigma_{g,18}$ ,  $\sigma_{g,31}$  lead to the bigger sum of DRESs’ output. The increase in the sum is biggest in  $\sigma_{g,31}$  followed by that of on  $\sigma_{g,6}$  and  $\sigma_{g,18}$ . The

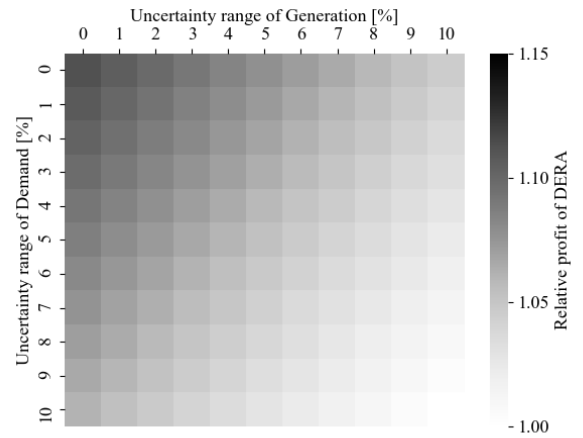


**FIGURE 12. Relative profit with various uncertainty ranges of generation and demand compared to a zero-uncertainty profit.**

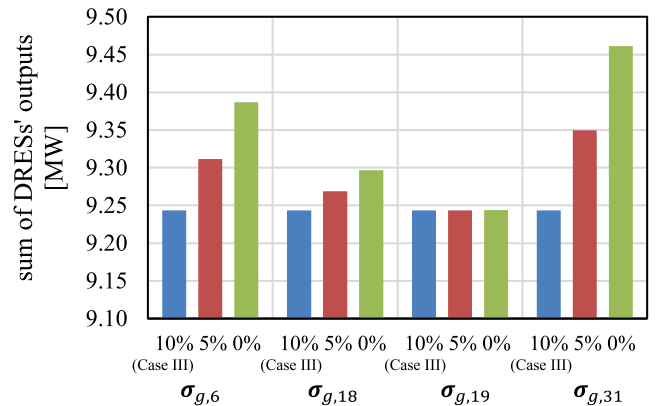


**FIGURE 13. Sum of output of DERA’s bid regarding the uncertainty range of generators on bus 6, 18, 19, and 31.**

reason can be inferred from the fact that  $p_{g,31}$ ,  $p_{g,6}$ , and  $p_{g,18}$  have different values in final step of Table 12.  $p_{g,31}$ ,  $p_{g,6}$ , and  $p_{g,18}$  are 2.40, 1.43, and 0.53 in MW respectively.

On the other hand, the uncertainty range of the WT on bus 19  $\sigma_{g,19}$  does not affect the sum of DRESs’ output. To find the reason for this, sensitivities to DRES outputs and activities of voltage and flow constraints need to be analyzed. Figure 14 shows voltages of risky buses and voltage sensitivities to the DRESs output on each bus. Figure 15 shows line usage rates and its sensitivities to the outputs of DRESs on each bus. In both figures, bigger sensitivities are colored darker and lower sensitivities are colored brighter in each row. It is shown that sensitivities of risky bus voltages to  $p_{g,19}$  are close to zero. Also, sensitivities of line usage rates on risky lines except line 18 to  $p_{g,19}$  are close to zero. For the usage rate of line 18 of which sensitivity to  $p_{g,19}$  is not zero, it is still 85 % that flow constraint of line 18 is inactive. This means  $p_{g,19}$  is not curtailed because of the flow on line 18. Because of these reasons, changes in  $\sigma_{g,19}$  do not affect the sum of DRESs’ output.

In the long term, under the proposed prequalification process, the DERA has an incentive to predict the DRES output accurately and fulfill the submitted bid in real time.

Bus #	Voltage [p.u.]	DRES bus #									
		6	7	9	11	12	18	19	21	31	33
12	1.050	0.01	0.01	0.02	0.03	0.03	0.03	0.00	0.00	0.01	0.01
18	1.050	0.01	0.01	0.02	0.03	0.03	0.06	0.00	0.00	0.01	0.01
31	1.050	0.01	0.01	0.01	0.01	0.01	0.01	0.00	0.00	0.03	0.03
32	1.049	0.01	0.01	0.01	0.01	0.01	0.01	0.00	0.00	0.03	0.03
33	1.049	0.01	0.01	0.01	0.01	0.01	0.01	0.00	0.00	0.03	0.04

Brightness indicates the size of sensitivities for each row

FIGURE 14. Sensitivity of voltage to DRES output in  $\chi_V^4$ .

Line #	Line usage rate	DRES bus #									
		6	7	9	11	12	18	19	21	31	33
5	100%	7.0	7.0	6.8	6.7	6.7	6.7	0.0	0.0	6.7	6.7
18	85%	0.0	0.0	0.0	0.0	0.0	0.0	4.1	4.1	0.0	0.0
22	92%	0.0	0.0	0.0	0.0	0.0	0.0	0.0	0.0	0.0	0.0
23	74%	0.0	0.0	0.0	0.0	0.0	0.0	0.0	0.0	0.0	0.0
30	86%	0.0	0.0	0.0	0.0	0.0	0.0	0.0	0.0	4.0	4.0

Brightness indicates the size of sensitivities for each row

FIGURE 15. Sensitivity of line usage rate to DRES output in  $\chi_F^4$ .

In addition, the proposed method can give conservative DSOs an incentive to overestimate the uncertainty in DERA’s resources. Therefore, it is important for the DSO to accurately and properly assess the uncertainty of DRES and demand not only to ensure robustness but also to ensure that the profit of the DERA is not suppressed.

VI. CONCLUSION

The participation of DERA in power markets using DRESs requires additional information exchange between the DSO and the DERA. The proposed prequalification process enables coordination between the minimal DSO and the DERA. The minimal DSO cannot directly dispatch the resources in its jurisdiction. Because DERA resources are variable DRESs, the DSO should consider the uncertainty of DRESs as the DSO manages its system.

Compared to the brute-force search method, the proposed prequalification method enables the DSO to maintain a robust distribution system in a more efficient manner. The proposed method is as robust as and much faster than the brute-force search method.

To verify the robustness of the proposed prequalification method, Monte Carlo simulations are conducted using the IEEE 33-bus distribution network under three cases. The results demonstrate that the proposed scheme is sufficiently robust for the expected uncertainty ranges. However, it is observed that it is important for the DSO to assess the uncertainties in its system properly. Overestimation can needlessly decrease the profit of a DERA, and underestimation can lead to overvoltage and overflow problems in the distribution system.

In contrast, even though the DSO does not know the bidding strategy of the DERA, it can guide the DERA bid using the bid-modification guideline. Furthermore, the guideline

does not include full network information; instead, it includes just the violations and sensitivities, which are linear constraints.

The proposed algorithm helps the minimal DSO maintain a robust distribution system while allowing a new entity to be introduced to the distribution system. The proposed algorithm can be applied only to a distribution system with a single DERA. Therefore, further researches are necessary with respect to the prequalification algorithm that can be applied to multiple DERAs in a single distribution system. In addition, the further researches should consider the DERAs that aggregate non-renewable distributed generators and electrical energy storage, taking into account multiple time steps and inter-temporal constraints.

REFERENCES

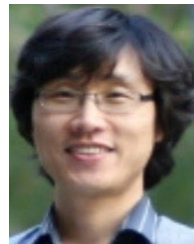
- [1] *Global Energy Transformation: A Roadmap to 2050*, IRENA, Abu Dhabi, UAB, 2018.
- [2] S. Burger, J. P. Chaves-Ávila, C. Batlle, and I. J. Pérez-Arriaga, “A review of the value of aggregators in electricity systems,” *Renew. Sustain. Energy Rev.*, vol. 77, pp. 395–405, Sep. 2017.
- [3] C. Eid, P. Codani, Y. Perez, J. Reneses, and R. Hakvoort, “Managing electric flexibility from distributed energy resources: A review of incentives for market design,” *Renew. Sustain. Energy Rev.*, vol. 64, pp. 237–247, Oct. 2016.
- [4] J. Wang, H. Zhong, W. Tang, R. Rajagopal, Q. Xia, C. Kang, and Y. Wang, “Optimal bidding strategy for microgrids in joint energy and ancillary service markets considering flexible ramping products,” *Appl. Energy*, vol. 205, pp. 294–303, Nov. 2017.
- [5] Y. Zhou, Z. Wei, G. Sun, K. W. Cheung, H. Zang, and S. Chen, “A robust optimization approach for integrated community energy system in energy and ancillary service markets,” *Energy*, vol. 148, pp. 1–15, Apr. 2018.
- [6] A. Majzoubi and A. Khodaei, “Application of microgrids in providing ancillary services to the utility grid,” *Energy*, vol. 123, pp. 555–563, Mar. 2017.
- [7] *Participation of Distributed Energy Resource Aggregations in Markets Operated by Regional Transmission Organizations and Independent System Operators*, FERC, Washington, DC, USA, 2020.
- [8] H. Saboori, M. Mohammadi, and R. Taghe, “Virtual power plant (VPP), definition, concept, components and types,” in *Proc. Asia-Pacific Power Energy Eng. Conf.*, Mar. 2011, pp. 1–4.
- [9] J. O. Petinrin and M. Shaabanb, “Impact of renewable generation on voltage control in distribution systems,” *Renew. Sustain. Energy Rev.*, vol. 65, pp. 770–783, Nov. 2016.
- [10] J. D. Watson, N. R. Watson, D. Santos-Martin, A. R. Wood, S. Lemon, and A. J. V. Miller, “Impact of solar photovoltaics on the low-voltage distribution network in New Zealand,” *IET Gener., Transmiss. Distrib.*, vol. 10, no. 1, pp. 1–9, Jan. 2016.
- [11] J. Wang, C. Chen, and X. Lu, “Guidelines for implementing advanced distribution management systems-requirements for DMS integration with DERMS and microgrids,” Argonne Nat. Lab., Argonne, IL, USA, Tech. Rep. ANL/ESD-15/15, 2015.
- [12] P. D. Martini, L. Kristov, M. Higgins, M. Asano, J. Taft, and E. Beeman, “Coordination of distributed energy resources; international system architecture insights for future market design,” Austral. Energy Market Operator, Melbourne, VIC, Australia, May 2018. Accessed: Nov. 12, 2020. [Online]. Available: <https://www.aemo.com.au/-/media/Files/Electricity/NEM/DER/2019/OEN/Newport-Intl-Review-of-DER-Coordination-for-AEMO-final-report.pdf>
- [13] *Distributed Energy Resources Market Design Concept Proposal*, NYISO, New York, NY, USA, 2017.
- [14] H. Gerard, E. I. Rivero Puente, and D. Six, “Coordination between transmission and distribution system operators in the electricity sector: A conceptual framework,” *Utilities Policy*, vol. 50, pp. 40–48, Feb. 2018.
- [15] L. Kristov, P. De Martini, and J. D. Taft, “A tale of two visions: Designing a decentralized transactive electric system,” *IEEE Power Energy Mag.*, vol. 14, no. 3, pp. 63–69, May 2016.
- [16] G. Boyd, “SPEN DSO vision,” *CIREN-Open Access Proc. J.*, vol. 2017, no. 1, pp. 2007–2010, 2017.



- [17] B. Cornélusse, D. Vangulick, M. Glavic, and D. Ernst, "A process to address electricity distribution sector challenges: The gedror project approach," in *Proc. Int. Conf. Electr. Distrib. (CIRED)*, 2015, paper 0449.
- [18] E. Rivero, D. Six, and H. Gerard, "Basic schemes for TSO-DSO coordination and ancillary services provision," in *Proc. EU Horizon SmartNet Project*, Feb. 2016, p. 12.
- [19] M. Farrokhsersht, N. G. Paterakis, M. Gibescu, Y. Tohidi, and J. G. Sloopweg, "A survey on the participation of distributed energy resources in balancing markets," in *Proc. 15th Int. Conf. Eur. Energy Market (EEM)*, Jun. 2018, pp. 1–5.
- [20] R. Brazier et al., "TSO-DSO report: An integrated approach to active system management with the focus on TSO-DSO coordination in congestion management and balancing," ENTSO-E, EDSO, EURELECTRIC, CEDEC, GEODE, 2019. Accessed: Nov. 12, 2020. [Online]. Available: [https://docstore.entsoe.eu/Documents/Publications/Position%20papers%20and%20reports/TSO-DSO\\_ASM\\_2019\\_190416.pdf](https://docstore.entsoe.eu/Documents/Publications/Position%20papers%20and%20reports/TSO-DSO_ASM_2019_190416.pdf)
- [21] F. Wang, X. Ge, P. Yang, K. Li, Z. Mi, P. Siano, and N. Duić, "Day-ahead optimal bidding and scheduling strategies for DER aggregator considering responsive uncertainty under real-time pricing," *Energy*, vol. 213, Dec. 2020, Art. no. 118765.
- [22] X. Lu, K. Li, F. Wang, Z. Mi, R. Sun, X. Wang, and J. Lai, "Optimal bidding strategy of DER aggregator considering dual uncertainty via information gap decision theory," *IEEE Trans. Ind. Appl.*, vol. 57, no. 1, pp. 158–169, Jan. 2021.
- [23] S. Abapour, B. Mohammadi-Ivatloo, and M. T. Hagh, "Robust bidding strategy for demand response aggregators in electricity market based on game theory," *J. Cleaner Prod.*, vol. 243, Jan. 2020, Art. no. 118393.
- [24] P. Sheikhhahmadi and S. Bahramara, "The participation of a renewable energy-based aggregator in real-time market: A Bi-level approach," *J. Cleaner Prod.*, vol. 276, Dec. 2020, Art. no. 123149.
- [25] P. Cuffe, P. Smith, and A. Keane, "Capability chart for distributed reactive power resources," *IEEE Trans. Power Syst.*, vol. 29, no. 1, pp. 15–22, Jan. 2014.
- [26] L. Ageeva, M. Majidi, and D. Pozo, "Analysis of feasibility region of active distribution networks," in *Proc. Int. Youth Conf. Radio Electron., Electr. Power Eng. (REEPE)*, Mar. 2019, pp. 1–5.
- [27] J. Silva, J. Sumaili, R. J. Bessa, L. Seca, M. A. Matos, V. Miranda, M. Caujolle, B. Goncer, and M. Sebastian-Viana, "Estimating the active and reactive power flexibility area at the TSO-DSO interface," *IEEE Trans. Power Syst.*, vol. 33, no. 5, pp. 4741–4750, Sep. 2018.
- [28] S. Riaz and P. Mancarella, "On feasibility and flexibility operating regions of virtual power plants and TSO/DSO interfaces," in *Proc. IEEE Milan PowerTech*, Jun. 2019, pp. 1–6.
- [29] D. Mayorga Gonzalez, J. Hachenberger, J. Hinker, F. Rewald, U. Häger, C. Rehtanz, and J. Myrzik, "Determination of the time-dependent flexibility of active distribution networks to control their TSO-DSO interconnection power flow," in *Proc. Power Syst. Comput. Conf. (PSCC)*, Jun. 2018, pp. 1–8.
- [30] P. Sheikhhahmadi, S. Bahramara, A. Mazza, G. Chicco, and J. P. S. Catalão, "Bi-level optimization model for the coordination between transmission and distribution systems interacting with local energy markets," *Int. J. Electr. Power Energy Syst.*, vol. 124, Jan. 2021, Art. no. 106392.
- [31] J. Hu, Y. Li, and H. Zhou, "Energy management strategy for a society of prosumers under the IOT environment considering the network constraints," *IEEE Access*, vol. 7, pp. 57760–57768, 2019.
- [32] P. Moutis, P. S. Georgilakis, and N. D. Hatziaargyriou, "Voltage regulation support along a distribution line by a virtual power plant based on a center of mass load modeling," *IEEE Trans. Smart Grid*, vol. 9, no. 4, pp. 3029–3038, Jul. 2018.
- [33] D. Pudjianto, G. Strbac, and D. Boyer, "Virtual power plant: Managing synergies and conflicts between transmission system operator and distribution system operator control objectives," *CIRED-Open Access Proc. J.*, vol. 2017, no. 1, pp. 2049–2052, Oct. 2017.
- [34] H. Fu, Z. Wu, X.-P. Zhang, and J. Brandt, "Contributing to DSO's energy-reserve pool: A chance-constrained two-stage  $\mu$  VPP bidding strategy," *IEEE Power Energy Technol. Syst. J.*, vol. 4, no. 4, pp. 94–105, Oct. 2017.
- [35] S.-W. Park and S.-Y. Son, "Interaction-based virtual power plant operation methodology for distribution system operator's voltage management," *Appl. Energy*, vol. 271, Aug. 2020, Art. no. 115222.
- [36] Q. Lu, Y. Yang, Y. Zhu, T. Xu, W. Wu, and J. Chen, "Distributed economic dispatch for active distribution networks with virtual power plants," in *Proc. IEEE Innov. Smart Grid Technol. Asia (ISGT Asia)*, May 2019, pp. 328–333.
- [37] Z. Yi, Y. Xu, J. Zhou, W. Wu, and H. Sun, "Bi-level programming for optimal operation of an active distribution network with multiple virtual power plants," *IEEE Trans. Sustain. Energy*, vol. 11, no. 4, pp. 2855–2869, Oct. 2020.
- [38] D. Koraki, J. Keukert, and K. Strunz, "Congestion management through coordination of distribution system operator and a virtual power plant," in *Proc. IEEE Manchester PowerTech*, Jun. 2017, pp. 1–6.
- [39] D. Koraki and K. Strunz, "Wind and solar power integration in electricity markets and distribution networks through service-centric virtual power plants," *IEEE Trans. Power Syst.*, vol. 33, no. 1, pp. 473–485, Jan. 2018.
- [40] H. S. Moon, S. W. Kim, and Y. G. Jin, "Alternative structure of distribution sector for neutral distribution system operation in Korea," in *Proc. 25th Int. Conf. Electr. Distrib. (CIRED)*, 2019, p. 922.
- [41] G. de Jong, O. Franz, P. Hermans, and M. Lallemand, "TSO-DSO data management report," TSO-DSO Project Team, ENTSO-E, EDSO, EURELECTRIC, CEDEC, GEODE, Tech. Rep., 2019. Accessed: Nov. 12, 2020. [Online]. Available: [http://www.edsoforsmartgrids.eu/wp-content/uploads/TSO-DSO\\_Data-management-Report.pdf](http://www.edsoforsmartgrids.eu/wp-content/uploads/TSO-DSO_Data-management-Report.pdf)
- [42] S. Küfeoğlu, S. W. Kim, and Y. G. Jin, "History of electric power sector restructuring in South Korea and Turkey," *Electr. J.*, vol. 32, no. 10, Dec. 2019, Art. no. 106666.
- [43] Y. H. Song, H. J. Kim, S. W. Kim, Y. G. Jin, and Y. T. Yoon, "How to find a reasonable energy transition strategy in Korea?: Quantitative analysis based on power market simulation," *Energy Policy*, vol. 119, pp. 396–409, Aug. 2018.
- [44] H. Saadat, *Power System Analysis*, vol. 2. New York, NY, USA: McGraw-Hill, 1999.
- [45] M. E. Baran and F. F. Wu, "Network reconfiguration in distribution systems for loss reduction and load balancing," *IEEE Power Eng. Rev.*, vol. 9, no. 4, pp. 101–102, Apr. 1989.
- [46] S. Kim, J. Kim, Y. Jin, and Y. Yoon, "Optimal bidding strategy for renewable microgrid with active network management," *Energies*, vol. 9, no. 1, p. 48, Jan. 2016.



**HEE SEUNG MOON** (Student Member, IEEE) received the B.S. degree in electrical and computer engineering from Seoul National University, Seoul, South Korea, in 2016, where he is currently pursuing the Ph.D. degree in electrical and computer engineering. His research interests include power economics, distribution system operation, balancing cost, and virtual power plant.



**YOUNG GYU JIN** (Member, IEEE) received the B.S., M.S., and Ph.D. degrees in electrical engineering from Seoul National University, in 1999, 2001, and 2014, respectively. From 2002 to 2010, he worked with KT Inc. He is currently an Associate Professor with the Department of Electrical Engineering, Jeju National University, South Korea. His research interests include optimal operation of smart grid/microgrid, renewable energy, and evolution of electrical grid.



**YONG TAE YOON** (Member, IEEE) received the B.S., M.Eng., and Ph.D. degrees from M.I.T., Cambridge, MA, USA, in 1995, 1997, and 2001, respectively. He is currently a Professor with the Department of Electrical and Computer Engineering, Seoul National University, Seoul, South Korea. His research interests include power economics, smart grid/microgrid, and decentralized operation.



**SEUNG WAN KIM** (Member, IEEE) received the B.S. and Ph.D. degrees in electrical engineering from Seoul National University, Seoul, South Korea, in 2012 and 2018, respectively. He is currently an Assistant Professor with the Department of Electrical Engineering, Chungnam National University, Daejeon, South Korea. His research interests include energy policy and electricity market design.

...